Semiclassical solitons in strongly correlated systems of ultracold bosonic atoms in optical lattices

Eugene Demler [a,*], Andrei Maltsev [b]

[a] Department of Physics, Harvard University, Cambridge, MA 02138, USA
[b] L.D. Landau Institute for Theoretical Physics, Chernogolovka, Moscow Reg. 142432, Russia

ARTICLE INFO

ABSTRACT

We investigate theoretically soliton excitations and dynamics of their formation in strongly correlated systems of ultracold bosonic atoms in two and three dimensional optical lattices. We derive equations of nonlinear hydrodynamics in the regime of strong interactions and incommensurate fillings, when atoms can be treated as hard core bosons. When parameters change in one direction only we obtain Korteweg–de Vries type equation away from half-filling and modified KdV equation at half-filling. We apply this general analysis to a problem of the decay of the density step. We consider stability of one dimensional solutions to transverse fluctuations. Our results are also relevant for understanding nonequilibrium dynamics of lattice spin models.

© 2011 Published by Elsevier Inc.

1. Introduction

Solitons are conspicuous manifestations of nonlinear interactions in a variety of physical systems (see e.g. [50,71]). Originally introduced in hydrodynamics of classical fluids, they were later observed in a variety of other systems, including plasma physics, nonlinear optics, magnetism, dynamics of molecular systems. It is currently understood that formation of oscillatory zones and localized solitonic solutions is a common feature of many non-linear systems and does not depend on the exact integrability of the model. However the character of solitons is different for each system and understanding their properties remains a fundamental problem in physics and mathematics.

In this paper we investigate theoretically the nature of solitons and dynamics of their formation in strongly correlated systems of ultracold bosonic atoms in optical lattices [11–13,41,60]. Recently questions of far from equilibrium many-body dynamics took central stage in both theoretical and

* Corresponding author.
  E-mail address: demler@physics.harvard.edu (E. Demler).

experimental study of ultracold atoms. What makes such systems particularly well suited for exploring quantum dynamics is their good isolation from the environment. Their characteristic energies and frequencies are of the order of kiloHertz, which is extremely convenient for experimental studies. It is also important that a wide array of experimental tools that allow to control system parameters in time and prepare far from equilibrium initial states have been developed. Recent experiments addressed such question as dynamics of fermions in optical lattices [86,82], observation of superexchange interactions using spin dynamics [89], thermalization and relaxation in one-dimensional systems [49,36,33], motion of impurity particles [52], dynamics and adiabaticity in crossing classical and quantum phase transitions [76,79]. Another important recent achievement is development of experimental tools for the in situ imaging of individual atoms in optical lattices [5,26,29,37,44,68,72,85] and low dimensional condensates [35,100]. This technique allows unprecedented level of characterization of many-body states and should lead to deeper understanding of their out of equilibrium dynamics. One example is recent analysis of Bakr et al. [5] of the dynamics of defect creation in crossing from the SF to Mott state in two dimensional optical lattices.

We start our analysis by deriving hydrodynamical approach to describe quantum dynamics of the lattice bosons. Hydrodynamical description has been applied to quantum many-body systems previously, including superfluids [47], superconductors [30], quantum Hall systems [91], and magnets [34]. The focus of most earlier analysis was on understanding collective modes and universal features of linear response functions, which only required understanding linear hydrodynamics. When non-linear effects have been discussed for superfluid systems, it was primarily done for systems in the continuum with the full Galilean symmetry. Our goal will be to include both nonlinearities and dispersion, since the competition of the two determines the nature and dynamics of solitons.

Solitons in systems of ultracold atoms have been discussed previously in the regimes where semiclassical Gross–Pitaevskii equation can be applied either in uniform systems [14,18,48,74,15] or systems with optical lattices [21,88,2,3,93,42,46]. In this paper we will be interested in the regime of very strong interactions between atoms, the so-called hard core bosons regime [80,83]. In this case dynamics of atoms in a lattice can be described using anisotropic Heisenberg model [80]. We demonstrate that in this regime the character of soliton excitations is very different and depends on both the filling factor and parameters of the Heisenberg model. Numerical analysis of solitons in Bose systems in optical lattices in the vicinity of the SF/Mott transition has been done recently by Krutitsky et al. [54]. Our results can also be applied to study nonequilibrium spin dynamics of two component Bose mixtures in the Mott insulating regime [20,51] and lattice spin systems in solid state physics.

2. Model

2.1. From lattice bosons to spin Hamiltonian

Microscopic model describing ultracold bosonic atoms in an optical lattice is given by the Bose–Hubbard model [41,12]

$$\mathcal{H}_{BH} = -t_b \sum_{\langle ij \rangle} b_i^\dagger b_j + \frac{U}{2} \sum_i n_i(n_i - 1). \tag{1}$$

Here $b_i^\dagger$ is a creation operator for bosons on site i, $n_i = b_i^\dagger b_i$ is the number of atoms on site i. We do not include the chemical potential term because in this paper we study dynamics and the operator of the total number of particles commutes with the Hamiltonian. It is sufficient to impose a certain number of particles at the initial time and then the total number of particles should not change during evolution. When there is inhomogeneous external potential we also need to add

$$V_{ext} = \sum_i V_i n_i \tag{2}$$

To keep the model more general we include nearest neighbor interactions

$$\mathcal{H}_{Ext\,BH} = \mathcal{H}_{Hub} + V \sum_{\langle ij \rangle} n_i n_j \tag{3}$$

Such non-local interactions are relevant for atoms in higher Bloch bands [81] and polar molecules in optical lattices [55]. We consider a regime when the local repulsion U is large and the density of particles is incommensurate with the lattice. In this case strong number fluctuations are suppressed even in the superfluid state and we can limit the Hilbert space to only two possible occupation numbers $|n_0 - 1\rangle$ and $|n_0\rangle$ per site. It is convenient to represent these states as spin states. State $|n_0 - 1\rangle_i$ corresponds to $|\downarrow\rangle_i$, and state $|n_0\rangle_i$ corresponds to $|\uparrow\rangle_i$. In this limit Hamiltonian (3) is equivalent to the anisotropic Heisenberg model

$$\mathcal{H}_{AH} = -J_\perp \sum_{\langle ij \rangle} \left(\sigma_i^x \sigma_j^x + \sigma_i^y \sigma_j^y \right) - J_z \sum_{\langle ij \rangle} \sigma_i^z \sigma_j^z \tag{4}$$

Here σ^a are Pauli matrices, $2J_\perp = t_b n_0$, and $J_z = -V$.

Hamiltonian (4) also appears as an effective description of spin dynamics in the Mott state of two component Bose mixtures at filling factor $n = 1$ [20,51].

2.2. Semiclassical equations of motion for lattice bosons

In this section we discuss how one can obtain semiclassical description of dynamics of (4) using either variational Gutzwiller wavefunctions or linearized equations of motion, which in this case are equivalent to lattice Landau–Lifshitz equations. To simplify the derivation we assume that parameters of the system change in one direction only. We emphasize that our focus is on two and three dimensional systems. Restriction to having variations of parameters in only one direction is, firstly, for notational simplicity (extension to higher dimensions is straightforward) and, secondly, because we will be concerned with problems where initial state has been prepared to have parameters changing along one of the coordinates. We discuss effects of fluctuations in transverse directions in subsequent sections.

Strictly one dimensional systems are special and mean-field approaches do not apply to them even in equilibrium. However special analytical approaches are available for one dimensional systems, including fermionization and Bethe ansatz [24,28,87]. Also powerful numerical methods based on DMRG [84] and Matrix Product States [16] allow to study dynamics of one dimensional systems in great details. On the other hand, nonequilibrium dynamics of higher dimensional systems remains largely unexplored. This is the main motivation for the current paper. Interestingly, recent work by Lancaster and Mitra [56] showed that semiclassical analysis of Landau–Lifshitz equations for one dimensional spin chains give results consistent with exact calculations. Hence our results may also be relevant for one dimensional spin chains.

To obtain semiclassical dynamics we consider time-dependent variational wavefunctions

$$|\Psi(t)\rangle = \prod_i \left[\sin\frac{\theta_i(t)}{2} e^{-i\varphi_i(t)/2} |\downarrow\rangle_i + \cos\frac{\theta_i(t)}{2} e^{i\varphi_i(t)/2} |\uparrow\rangle_i \right] \tag{5}$$

Expectation values of the original boson operators are

$$\langle b_i \rangle = \frac{\sqrt{n_0}}{2} \sin\theta_i e^{-i\varphi_i}$$
$$\langle n_i \rangle = n_0 + \frac{1}{2}(\cos\theta_i - 1) \tag{6}$$

To project Schrödinger equation into wavefunction (5) we define the Lagrangian [40,39]

$$L = -i\left\langle \Psi \left| \frac{d}{dt} \right| \Psi \right\rangle + \langle \Psi | H | \Psi \rangle$$
$$= \sum_i \frac{1}{2}\dot{\varphi}_i \cos\theta_i - J_\perp \sum_{\langle ij \rangle} \sin\theta_i \sin\theta_j \cos(\varphi_i - \varphi_j) - J_z \sum_{\langle ij \rangle} \cos\theta_i \cos\theta_j$$

and write equations of motion

$$\frac{d}{dt}\frac{\delta L}{\delta \dot{q}_i} - \frac{\delta L}{\delta q_i} = 0 \tag{7}$$

Here q_i corresponds to both φ_i and θ_i. We find

$$
\begin{aligned}
\dot{\varphi}_i \sin\theta_i &= -4J_\perp \cos\theta_i\big(\sin\theta_{i+1}\cos(\varphi_i - \varphi_{i+1}) + \sin\theta_{i-1}\cos(\varphi_i - \varphi_{i-1})\big) \\
&\quad + 4J_z \sin\theta_i(\cos\theta_{i+1} + \cos\theta_{i-1}) \\
\dot{\theta}_i &= -4J_\perp\big(\sin\theta_{i+1}\sin(\varphi_i - \varphi_{i+1}) + \sin\theta_{i-1}\sin(\varphi_i - \varphi_{i-1})\big)
\end{aligned}
\tag{8}
$$

The first equation is effectively the Josephson relation: time derivative of the phase φ is equal to the chemical potential which depends on the values of θ and φ. The second equation is charge conservation.

One can give an alternative physical interpretation to Eqs. (8). We write equations of motion for spin operators

$$
\frac{d\sigma_i^x}{dt} = -2J_\perp \sigma_i^z(\sigma_{i-1}^y + \sigma_{i+1}^y) + 2J_z \sigma_i^y(\sigma_{i-1}^z + \sigma_{i+1}^z) + h_z^i \sigma_i^y
\tag{9}
$$

And we have analogous equations for $\sigma_i^{\{y,z\}}$. To obtain semiclassical dynamics we replace operators by their expectation values

$$
\frac{d\langle\sigma_i^x\rangle}{dt} = -2J_\perp\langle\sigma_i^z\rangle\big(\langle\sigma_{i-1}^y\rangle + \langle\sigma_{i+1}^y\rangle\big) + 2J_z\langle\sigma_i^y\rangle\big(\langle\sigma_{i-1}^z\rangle + \langle\sigma_{i+1}^z\rangle\big) + B_z^i\langle\sigma_i^y\rangle
\tag{10}
$$

These are familiar Landau–Lifshitz equations. If we use wavefunction (5) to calculate $\langle\sigma_i^z\rangle = \cos\theta_i$ and $\langle\sigma_i^+\rangle = \frac{1}{2}\sin\theta_i e^{-i\varphi_i}$, we recognize that Landau–Lifshitz equations are equivalent to (8).

Dynamics of the Bose–Hubbard model has been studied using Gutzwiller variational wavefunctions in [99,17,66,38]. In [4,75] this approach was used to describe current decay in the strongly interacting regime of bosons. Theoretical predictions were in quantitative agreement with subsequent experimental results by Mun et al. [65].

3. Semiclassical dynamics in the continuum limit

3.1. Long wavelength expansion

It is convenient to introduce slow variables in space, $X = hx$, and time, $T = ht$, where h is the lattice constant. We are looking at dynamics of fluctuations that are slow on the scale of the lattice constant. So h is a small parameter in which we will expand. We introduce

$$
\begin{aligned}
\mu &= \cos\theta \\
\sigma(X,T) &= h\varphi(X,t)
\end{aligned}
\tag{11}
$$

and obtain

$$
\begin{aligned}
\mathcal{L} &= \frac{1}{2}\sigma_T\mu - 2J_\perp(1-\mu^2)\cos\sigma_X - 2J_z\mu^2 + h^2 J_\perp \frac{\mu^2\mu_X^2}{1-\mu^2}\cos\sigma_X + h^2 J_\perp(1 \\
&\quad - \mu^2)\Big(\frac{1}{3}\sigma_{XXX}\sin\sigma_X + \frac{1}{4}\sigma_{XX}^2\cos\sigma_X\Big) - h^2 J_z\mu\mu_{XX} + \mathcal{O}(h^4)
\end{aligned}
\tag{12}
$$

3.2. Hydrodynamics

If we keep only the lowest order terms in h in (12), we obtain the hydrodynamic part of the lagrangian

$$
\mathcal{L}_{Hydr} = \frac{1}{2}\sigma_T\mu - 2J_\perp(1-\mu^2)\cos\sigma_X - 2J_z\mu^2
\tag{13}
$$

It is convenient to define

$$
k(X,T) = \sigma_X(X,T)
\tag{14}
$$

The new variable is proportional to the phase gradient, $k \sim \nabla\varphi$.

Equations of motion obtained from the lagrangian (13) have a standard hydrodynamic form

$$k_T = 8J_\perp \mu \sin k k_X - (8J_\perp \cos k - 8J_z)\mu_X$$
$$\mu_T = -4J_\perp(1 - \mu^2)\cos k k_X + 8J_\perp \mu \sin k \mu_X$$

(15)

3.3. Linearized equations of motion. Stable and unstable regimes

Let us consider a superfluid state with a uniform density and, possibly, finite phase winding. When $k \neq 0$, this is a current carrying state with $I = 4J_\perp(1 - \mu_0^2)\sin k$.

Frequencies of linearized excitations are given by the eigenvalues of the matrix

$$A = \begin{pmatrix} 8J_\perp \mu \sin k & -8J_\perp \cos k + 8J_z \\ -4J_\perp(1 - \mu^2)\cos k & 8J_\perp \mu \sin k \end{pmatrix}$$

(16)

We have for the eigenvalues of A

$$\lambda_{1,2} = 8J_\perp \mu \sin k \pm \sqrt{4J_\perp(1 - \mu^2)\cos k(8J_\perp \cos k - 8J_z)}$$

(17)

When $J_\perp > J_z$ and k is small, both eigenvalues of (16) are real (when $J_z = 0$ this is true for all k). This is the hyperbolic regime, which will be the main focus of our paper.

When $0 < \cos k < J_z/J_\perp$, eigenvalues of (16) appear as a complex conjugate pair. This is the elliptic regime, which corresponds to the unstable state of the system. In this regime small fluctuations of the plane wave type

$$k(X,T) = k_0 + \delta k(X,T), \quad \mu(X,T) = \mu_0 + \delta\mu(X,T)$$
$$\delta k(X,T) \sim \delta k e^{iqX+iv(q)T}, \quad \delta\mu(X,T) \sim \delta\mu e^{iqX+iv(q)T}$$

grow exponentially in time. Existence of this unstable regime is known as the dynamical instability [92,4]. It was observed experimentally for atoms in optical lattices [22,65]. Exponential growth of small modulations predicted by Eq. (15) is only valid for short times. Dynamics of the unstable regime beyond the short time limit can be analyzed using mathematical methods from the theory of elliptic equations. In this paper we only address the stable hyperbolic regime.

When the initial state does not carry a current, i.e. there is no phase winding,

$$\varphi(X,0) = 0$$

(18)

To obtain further insight into the linearized system we set

$$\mu(X,T) = \mu_0 + \rho(X,T)$$

We can now rewrite Eq. (15) in terms of variables $\rho(X,T)$ and $k(X,T)$, which describe small deviations from the equilibrium state

$$k_T = -8(J_\perp - J_z)\rho_X, \quad \rho_T = -4J_\perp(1 - \mu_0^2)k_X$$

(19)

System (19) gives the following equation for $\rho(X,T)$

$$\rho_{TT} = 32J_\perp(1 - \mu_0^2)(J_\perp - J_z)\rho_{XX}$$

(20)

We find the familiar wave equation, which describes propagation of the initial perturbation $\rho(X,0)$ with a small amplitude. Eqs. (19) and (20) show that during the dynamical evolution of the perturbation, the superfluid velocity $k(X,T)$ is of the order of $\rho(X,T)$, provided that this is true in the initial state. This is the regime that will be the focus of our paper.

3.4. Nonlinearities and appearance of singularities

We now include nonlinear terms in the analysis of equations of motion. In the simplest case $J_z = 0$ we can define

$$
\begin{aligned}
r^1 &= \sqrt{2}\arcsin\mu - k = \pi/\sqrt{2} - \sqrt{2}\theta - k \\
r^2 &= \sqrt{2}\arcsin\mu + k = \pi/\sqrt{2} - \sqrt{2}\theta + k
\end{aligned}
\tag{21}
$$

And from the Lagrangian (13) we obtain equations of motion

$$
\begin{aligned}
r_T^1 &= \left(8J_\perp \sin\frac{r^1 + r^2}{2\sqrt{2}} \sin\frac{r^2 - r^1}{2} + 4\sqrt{2}J_\perp \cos\frac{r^1 + r^2}{2\sqrt{2}} \cos\frac{r^2 - r^1}{2} \right) r_X^1 \\
r_T^2 &= \left(8J_\perp \sin\frac{r^1 + r^2}{2\sqrt{2}} \sin\frac{r^2 - r^1}{2} - 4\sqrt{2}J_\perp \cos\frac{r^1 + r^2}{2\sqrt{2}} \cos\frac{r^2 - r^1}{2} \right) r_X^2
\end{aligned}
\tag{22}
$$

Eqs. (22) are written in terms of the Riemann invariants, which separate the system (15) into the left- and right-moving parts. This representation is most convenient in the analysis of Hydrodynamic Type systems. System of Eqs. (22) admits two natural reductions $r^1 = const$ or $r^2 = const$, which describe separate propagation of the left- and right-moving excitations.

When $J_z \neq 0$, expressions for Riemann invariants are more cumbersome

$$
r^{1,2} = \sqrt{2}\arcsin\mu - \sqrt{2}\arcsin\mu_0 \mp \int_0^k \frac{\sqrt{\cos k}}{\sqrt{\cos k - J_z/J_\perp}} dk
$$

The corresponding diagonal system of the equations of motion has a character close to (22) in the hyperbolic regime.

Taking in the account that the functions $\rho(X,T)$ and $k(X,T)$ have the same order in our approach we can write

$$
\begin{aligned}
\lambda_{1,2} = &\pm \sqrt{32(1 - \mu_0^2)J_\perp(J_\perp - J_z)} + 8J_\perp\mu_0 k \mp \frac{\mu_0}{\sqrt{1 - \mu_0^2}}\sqrt{32J_\perp(J_\perp - J_z)}\rho \\
&+ 8J_\perp\rho k \mp \sqrt{2(1 - \mu_0^2)J_\perp}\frac{2J_\perp - J_z}{\sqrt{J_\perp - J_z}}k^2 \mp \sqrt{8J_\perp(J_\perp - J_z)}\frac{1}{\left(\sqrt{1 - \mu_0^2}\right)^3}\rho^2 + \cdots
\end{aligned}
\tag{23}
$$

In the same way

$$
r^{1,2} = \frac{\sqrt{2}}{\sqrt{1 - \mu_0^2}}\rho + \frac{\sqrt{2}\mu_0}{\left(\sqrt{1 - \mu_0^2}\right)^3}\frac{\rho^2}{2} + \frac{\sqrt{2}(1 + 2\mu_0^2)}{\left(\sqrt{1 - \mu_0^2}\right)^5}\frac{\rho^3}{6} + \cdots \mp \frac{k}{\sqrt{1 - J_z/J_\perp}} \mp \frac{J_z}{12J_\perp\left(\sqrt{1 - J_z/J_\perp}\right)^3}k^3 \mp \cdots
\tag{24}
$$

To understand the role of non-linear effects we expand the corresponding equations of motion up to second order terms in deviations from the uniform state. We obtain the following general form of the equations of motion

$$
\begin{aligned}
r_T^1 &= \sqrt{J_\perp(J_\perp - J_z)}\left(\sqrt{32(1 - \mu_0^2)} - 6\mu_0 r^1 + 2\mu_0 r^2 \right) r_X^1 \\
r_T^2 &= \sqrt{J_\perp(J_\perp - J_z)}\left(-\sqrt{32(1 - \mu_0^2)} - 2\mu_0 r^1 + 6\mu_0 r^2 \right) r_X^2
\end{aligned}
\tag{25}
$$

Eq. (25) describes coupled evolution of the right and left moving parts. To get further insight into dynamics we make another simplification. In the problems that we consider the left and right moving parts overlap at short times, but separate after a finite time. The main effects of non-linearities appear at long times. Thus when discussing effects of non-linearities it is sufficient to consider separately the left- and right-moving parts of the solution. So when we discuss the dynamics of r^1 we can set $r^2 = const$ and vice versa.

After we make the Galilean transformation for the left and right propagating parts we obtain

$$r_T^1 = -6\mu_0\sqrt{J_\perp(J_\perp - J_z)}r^1 r_X^1 \tag{26}$$

$$r_T^2 = 6\mu_0\sqrt{J_\perp(J_\perp - J_z)}r^2 r_X^2 \tag{27}$$

Eqs. (26) and (27) are known as the Hopf equations describing "simple waves". Their solutions are given by the implicit formula

$$r^{1,2} = F\left(X \mp 6\mu_0\sqrt{J_\perp(J_\perp - J_z)}r^{1,2}T\right)$$

The most important feature of these solutions is that they exist only up to a finite time T_0, which depends on the initial conditions. All nontrivial solutions become singular after some finite time. Physically this corresponds to formation of the breaking point, which we show in Fig. 1. This can be understood as a result of regions of different densities moving with different velocities.

Formation of the singularity is not restricted to the truncated equations of motion (25). This is a feature of the general non-linear dynamics of the equations of motion (22). Generally system of Eqs. (15) can be reduced to a linear problem using the so-called hodograph transformation. Then solutions of (15) can be described in terms of perturbations moving along the characteristic lines $dX/dT = \lambda_{1,2}(r^1, r^2)$. Characteristics of the nonlinear system depend on the variables (r^1, r^2) and unique solutions of (15) exist only up to a finite time T_0. At later times solution becomes multi-valued. Special solutions of (15) given by relations $r^1(X,T) = const$ or $r^2(X,T) = const$ describe perturbations moving along one of the characteristic lines. In this case the second variable (r^2 or r^1) satisfies a nonlinear first order equation, which is (locally) equivalent to the nonlinear Hopf equation.

For times approaching T_0 solutions of (26) and (27) are close to developing a breaking point and have high gradients. In this regime neglecting higher order gradients in the Lagrangian (12) is no longer justified. In the next section we will see that taking dispersion into account suppresses singularities in the solutions and gives rise to short-period oscillations.

General analysis of how dispersion leads to the formation of oscillatory zones in our system is rather complicated. In the most generic case, one can not use expansion (12) to describe the oscillatory zone formation. The period of oscillations arising for $T > T_0$ is of the order of h, so all higher dispersive corrections are of the same order. Accurate description of the transition from the "slowly-modulated" to the rapidly modulated regimes can only be done with the use of the original lattice system (8). However, there are certain special cases, in which the use of the continuum model (12) is justified. Fortunately these cases are interesting from the experimental point of view. They will be the subject of our discussion.
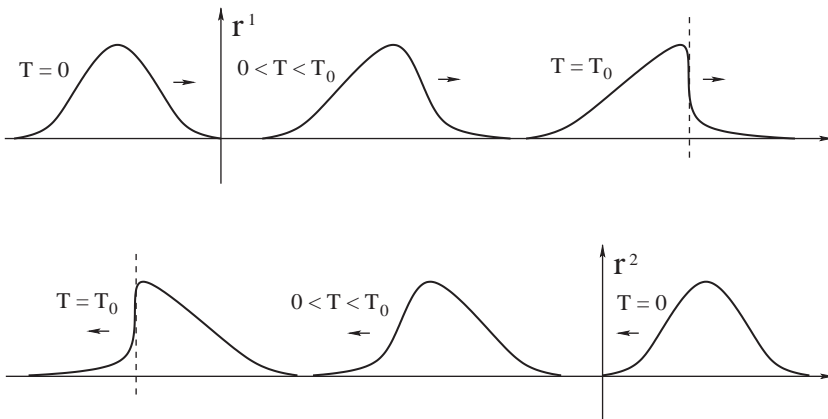
Fig. 1. Formation of the breaking point for Eqs. (26) and (27) in the case $\mu_0 > 0$. r^1 and r^2 describe left and right movers, respectively. Dynamics is shown in moving frames of references. In both cases the rear edge of the wave steepens and develops a singularity.

4. Nonlinear waves in generic case

4.1. Connection to Korteweg–de Vries equation

When discussing dispersive terms for ρ and k in the equations of motion, it is sufficient to keep them only in the linear order in deviations from the uniform state. Dispersive terms come with additional factors of h and are already small. Hence in the Lagrangian (12) dispersive terms need to be considered only up to quadratic terms in ρ or σ_X. Modulo total derivatives with respect to X we can write

$$\mathcal{L}_{Disp} \simeq h^2 J_\perp \frac{\mu_0^2}{1-\mu_0^2}\rho_X^2 + h^2 J_z \rho_X^2 - \frac{1}{12}h^2 J_\perp (1-\mu_0^2)\sigma_{XX}^2$$

The resulting equations of motion are

$$k_T \simeq 8J_\perp \mu \sin k k_X - (8J_\perp \cos k - 8J_z)\mu_X + 4h^2 J_\perp \frac{\mu_0^2}{1-\mu_0^2}\rho_{XXX} + 4h^2 J_z \rho_{XXX}$$

$$\mu_T \simeq -4J_\perp(1-\mu^2)\cos k k_X + 8J_\perp \mu \sin k \mu_X - \frac{1}{3}h^2 J_\perp(1-\mu_0^2)k_{XXX} \tag{28}$$

Using variables $r^1(k,\mu), r^2(k,\mu)$ we obtain

$$\begin{aligned} r_T^1 = &\sqrt{J_\perp(J_\perp - J_z)}\left(\sqrt{32(1-\mu_0^2)} - 6\mu_0 r^1 + 2\mu_0 r^2\right)r_X^1 \\ &- \frac{1}{3\sqrt{2}}h^2\sqrt{J_\perp(J_\perp - J_z)}\sqrt{1-\mu_0^2}(r_{XXX}^2 - r_{XXX}^1) \\ &- \sqrt{2}h^2\left(J_\perp \frac{\mu_0^2}{1-\mu_0^2} + J_z\right)\sqrt{1-\mu_0^2}\sqrt{\frac{J_\perp}{J_\perp - J_z}}(r_{XXX}^1 + r_{XXX}^2) \end{aligned} \tag{29}$$

$$\begin{aligned} r_T^2 = &\sqrt{J_\perp(J_\perp - J_z)}\left(-\sqrt{32(1-\mu_0^2)} - 2\mu_0 r^1 + 6\mu_0 r^2\right)r_X^2 \\ &- \frac{1}{3\sqrt{2}}h^2\sqrt{J_\perp(J_\perp - J_z)}\sqrt{1-\mu_0^2}(r_{XXX}^2 - r_{XXX}^1) \\ &+ \sqrt{2}h^2\left(J_\perp \frac{\mu_0^2}{1-\mu_0^2} + J_z\right)\sqrt{1-\mu_0^2}\sqrt{\frac{J_\perp}{J_\perp - J_z}}(r_{XXX}^1 + r_{XXX}^2) \end{aligned} \tag{30}$$

As in our earlier discussion we consider separately the left and right moving parts, i.e. we take either r^1 = const or r^2 = const. After we included effects of dispersion such reductions are no longer exact. However, in cases of interest, interaction between r^1 and r^2 gives rise only to small rapid oscillations. Such oscillations are expected to be much smaller than the structures that we discuss (see e.g. [53], see also [23,94,95]) and we will neglect them in this paper. We also perform Galilean transformations for the two parts and obtain in the moving coordinate systems

$$r_T^1 = -6\mu_0\sqrt{J_\perp(J_\perp - J_z)}r^1 r_X^1 + \sqrt{2}h^2\sqrt{1-\mu_0^2}\sqrt{\frac{J_\perp}{J_\perp - J_z}}\left(J_\perp\left(\frac{1}{6} - \frac{\mu_0^2}{1-\mu_0^2}\right) - \frac{7}{6}J_z\right)r_{XXX}^1 \tag{31}$$
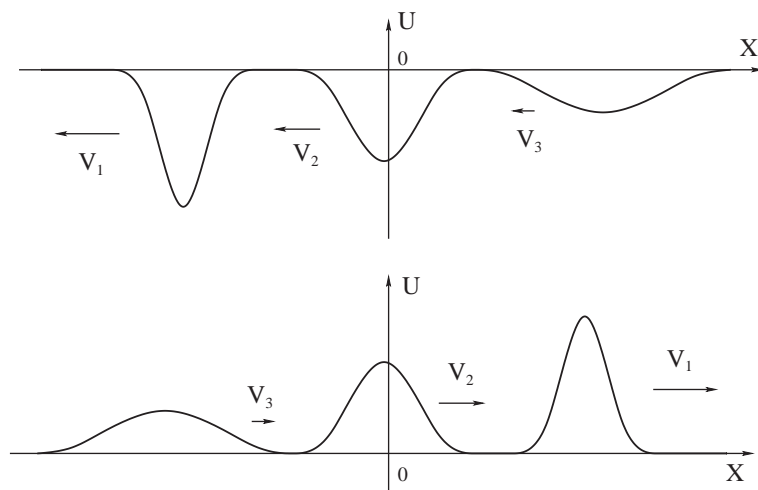
$$r_T^2 = 6\mu_0\sqrt{J_\perp(J_\perp - J_z)}r^2 r_X^2 - \sqrt{2}h^2\sqrt{1-\mu_0^2}\sqrt{\frac{J_\perp}{J_\perp - J_z}}\left(J_\perp\left(\frac{1}{6} - \frac{\mu_0^2}{1-\mu_0^2}\right) - \frac{7}{6}J_z\right)r_{XXX}^2 \tag{32}$$

Note that Eqs. (31) and (32) transform into each other if we change $X \to -X$. Equivalence of the two equations for fixed values of $J_\perp, J_z$ and μ_0 represents an evident corollary of the symmetry $X \to -X$ of the original system.

It is not difficult to see that Eqs. (31) and (32) represent the KdV-equation provided that

$$\mu_0 \neq 0, \quad J_\perp\left(\frac{1}{6} - \frac{\mu_0^2}{1-\mu_0^2}\right) - \frac{7}{6}J_z \neq 0$$

Fig. 2. The asymptotic form ($T \rightarrow \infty$) of the N-soliton solutions for Eqs. (33) and (34) respectively ($V_1 > V_2 > V_3$).

Depending on the values of parameters $J_\perp, J_z$, and μ_0, Eqs. (31) and (32) are equivalent to one of the following two equations

$$U_T + 6UU_X - U_{XXX} = 0 \tag{33}$$
$$U_T + 6UU_X + U_{XXX} = 0 \tag{34}$$

after an appropriate rescaling of coordinates (X, T) and functions r^i. These two equations are equivalent to each other if we admit the inversion $r^i \rightarrow -r^i$, $T \rightarrow -T$. However, this transformation leads to very different physical interpretation of solutions for a fixed μ_0, as we discuss below.[1]

KdV type equations (33) and (34) allow solitonic solutions, which are long lived nonlinear excitations in the system. The velocity of a soliton is proportional to its amplitude, so larger solitons move faster than the smaller ones. The asymptotic form of an N-soliton solution for $T \rightarrow \infty$ for Eqs. (33) and (34) can be represented as shown in Fig. 2. In the Appendix we briefly review how one can verify the existence of solitonic excitations in the KdV equation using connection to the linear Schrödinger equation. We also point out that in general, solutions of (33) and (34) include not only the soliton part but also "wave trains". The soliton part and the "wave train" parts separate from each other at long times (Fig. 3). The soliton part of the solution remains unchanged for all $T > 0$ while the wave - train part "dissolves" as $T \rightarrow \infty$ [96]. From our point of view, solitons of (33) and (34) represent the most interesting part of the solution and we focus on them in this paper.

### 4.2. Discussion of solitonic excitations

Solitons in KdV equations have been studied in detail during the last few decades. In this paper we take previously known mathematical results and discuss their physical implications for our specific system. While we provide a brief summary of the mathematical methods used in analyzing soliton excitations in the Appendix, we refer readers to the books [1,69,70] for a more detailed discussion of general mathematical aspects of the KdV equation.

The character of solitonic solutions of KdV type Eqs. (33) and (34) depends on parameters. In particular depending on the ratio of $J_z/J_\perp$ and the density, isolated solitons can appear either as particle-like or hole-like excitations. In this subsection we only provide a summary of the results. More details can be found in the Appendix.

---

[1] In the next chapter we will also discuss that solutions of (33) and (34) demonstrate different stability properties with respect to two-dimensional modulations.
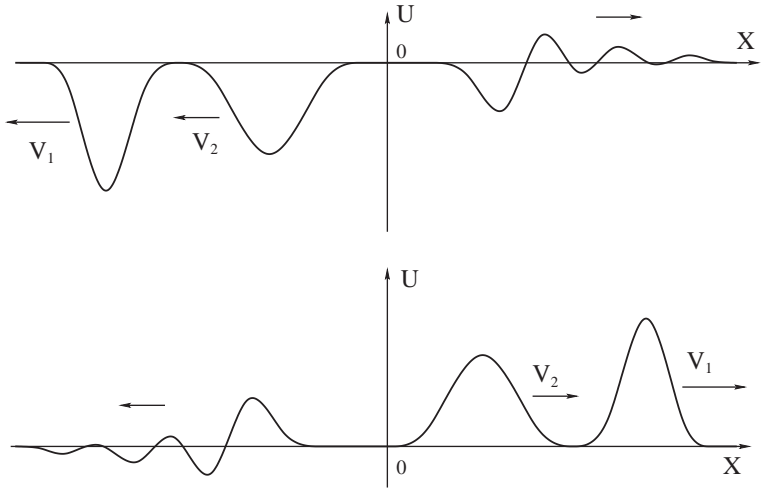
Fig. 3. The asymptotic form ($T \to \infty$) of the general solution for Eqs. (33) and (34) respectively.
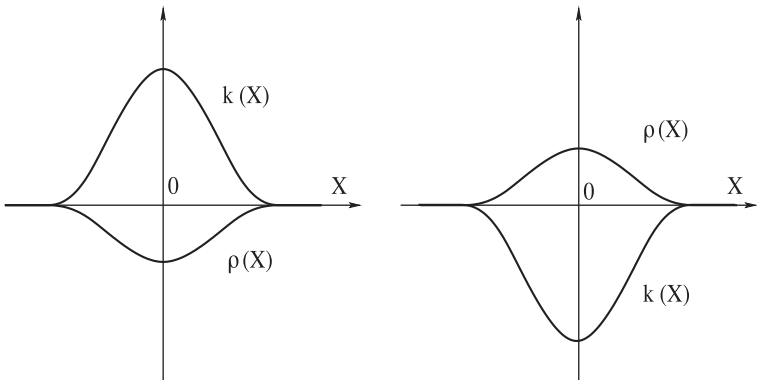
Fig. 4. The form of a soliton solution in the (k, ρ)-variables for the case of the "hole-like" soliton and the "particle-like" soliton, respectively.

In the discussion below we only consider the case $\mu_0 > 0$, which corresponds to the density above half-filling $\langle n \rangle > 1/2$. Eqs. (31) and (32) have a symmetry $\mu_0 \to -\mu_0$, $r_i \to -r_i$. This symmetry originates from the particle-hole symmetry of the initial system, which relates states below and above half-filling (8): $\theta \to \pi - \theta$ and $\varphi \to -\varphi$. In our discussion this symmetry allows to relate solitonic excitations below and above half-filling. For $\mu_0 < 0$ solitons are "mirror images" of the $\mu_0 > 0$ case. For example, if we find particle-like solitons above half-filling, we should have hole-like solitons below half-filling ($\mu_0 \to -\mu_0$) for the same values of J. Let us represent here also the form of the "hole-like" and the "particle-like" solitons in the original variables (k, ρ) (see Fig. 4).

We also remind the readers that we only need to consider states that are stable against dynamical modulations, i.e. $J_\perp > J_z$.

Solitons for $J_z > J_\perp/7$ and $\mu_0 > 0$

In this case both Eqs. (31) and (32) reduce to Eq. (34) after rescaling the variables and, if necessary, performing the transformation $X \to -X$. There should be no solitons when $U(X) \leqslant 0$. We are guaranteed to find solitonic excitations when

$$\int_{-\infty}^{+\infty} U(X)dX > 0 \qquad\qquad (35)$$

When $U(X) \geqslant 0$ the soliton part represents the main part of the solution. So we find particle-like solitons in this situation.

Solitons for $J_z < J_\perp/7$ and $0 < \mu_0 < \sqrt{\dfrac{J_\perp - 7J_z}{7(J_\perp - J_z)}}$

Now both Eqs. (31) and (32) reduce to Eq. (33) after rescaling the variables and doing the transformation $X \to -X$ in Eq. (32). This equation does not have any solitons when $U(X) \geqslant 0$. It has guaranteed solitonic solutions when

$$\int_{-\infty}^{+\infty} U(X)dX < 0 \qquad\qquad (36)$$

In the case with $U(X) \leqslant 0$ the soliton part represents the main part of the solution. Hence in terms of the original density, we find the hole-type solitons in this case.

Solitons for $J_z < J_\perp/7$ and $\sqrt{\dfrac{J_\perp - 7J_z}{7(J_\perp - J_z)}} < \mu_0 < 1$

Both Eqs. (31) and (32) reduce to Eq. (34) in this case. Thus we find particle-like solitons in terms of the original density.

We can now summarize results of this subsection. When $J_z > J_\perp/7$ we find that above half-filling there are only particle-like solitonic excitations. When $J_z < J_\perp/7$ and above half-filling we find that we have either hole-like (closer to half-filling) or particle-like solitons (closer to filling factor one).

4.3. Self-consistency of the long wavelength expansion

Before concluding this section we would like to verify that our solutions do not take us outside the region of applicability of Lagrangian (12), which was obtained using long wavelength expansion. When we consider dynamics starting from a state with small smooth deviations from a uniform density, approximate Lagrangian (12) can be certainly used at the initial stages of the evolution. However, at final (asymptotic) stages of the evolution, the solution may be sufficiently different from the initial state. Let us consider specifically the soliton part of asymptotic solutions. In soliton solutions both the nonlinear and dispersive parts are important and the interplay of the two gives rise to a stable soliton. One of the important properties of the KdV equation is that the amplitude of solitons is of the same order as initial deviations from the uniform density. Eqs. (31) and (32) were obtained assuming small deviations of the initial density from the uniform value μ_0. These small deviations set the scale for the amplitude of resulting solitons. In solitons there is a direct relation between the amplitude and the width (the width increases as the amplitude goes to zero). Hence in the limit that we discuss, the dispersion part of our soliton solutions should be small, and our approximation of neglecting higher dispersion corrections should be justified even for the final stages of the evolution. For example, when solution can be written as the "quasiclassical solution", in which the soliton part represents the main contribution to the solution, higher dispersive and nonlinear terms should have very weak effect on the soliton.

Similar considerations are applicable for the "wave-train" part of the solutions. However, the "wave-train" part dissolves in the limit $T \to \infty$ and we expect that it will be more challenging to observe it in experiments.

5. Nonlinear waves in special cases

5.1. Half-filling. Solitons of the modified Korteweg–de Vries equation

When the particle density is 1/2, the system of hard core bosons has a full particle-hole symmetry. Eigenvalues $\lambda_{1,2}$ of the linearized system (19) have the largest possible magnitude

$$\lambda_{1,2} = \pm 4\sqrt{2J_\perp(J_\perp - J_z)}$$

which corresponds to the largest possible velocity of linear waves. In the case of dynamics starting from some initial state, this should provide fastest spatial separation of the left- and right-moving parts of the perturbation. In this case $\mu_0 = 0$, so corrections to $\lambda_{1,2}$, which are linear in ρ and k, vanish and we need to use quadratic terms in the expansion (23). In our discussion below we keep linear terms, in order to accommodate small $\mu_0 \neq 0$. Using approximation (24) we can write

$$\lambda_1 \simeq \sqrt{J_\perp(J_\perp - J_z)} \left[4\sqrt{2} - 6\mu_0 r^1 + 2\mu_0 r^2 - \frac{7J_\perp - J_z}{2\sqrt{2}J_\perp}(r^1)^2 + \frac{J_\perp + J_z}{2\sqrt{2}J_\perp}(r^2)^2 + \frac{J_\perp - J_z}{2\sqrt{2}J_\perp} r^1 r^2 \right]$$

$$\lambda_1 \simeq \sqrt{J_\perp(J_\perp - J_z)} \left[-4\sqrt{2} - 2\mu_0 r^1 + 6\mu_0 r^2 - \frac{J_\perp + J_z}{2\sqrt{2}J_\perp}(r^1)^2 + \frac{7J_\perp - J_z}{2\sqrt{2}J_\perp}(r^2)^2 - \frac{J_\perp - J_z}{2\sqrt{2}J_\perp} r^1 r^2 \right]$$

From the last two equations we determine how propagation of the left- and right- moving parts, (31) and (32), is modified by the higher order terms. Within the assumptions of spatial separation of the left- and right-moving parts, which we used in the earlier discussion, and using appropriate moving frames of reference we find

$$r_T^1 = \sqrt{J_\perp(J_\perp - J_z)} \left(-6\mu_0 r^1 - \frac{7J_\perp - J_z}{2\sqrt{2}J_\perp}(r^1)^2 \right) r_X^1 + h^2 \sqrt{\frac{2J_\perp}{6(J_\perp - J_z)}}(J_\perp - 7J_z) r_{XXX}^1 \tag{37}$$

$$r_T^2 = \sqrt{J_\perp(J_\perp - J_z)} \left(6\mu_0 r^2 + \frac{7J_\perp - J_z}{2\sqrt{2}J_\perp}(r^2)^2 \right) r_X^2 - h^2 \sqrt{\frac{2J_\perp}{6(J_\perp - J_z)}}(J_\perp - 7J_z) r_{XXX}^2 \tag{38}$$

In writing the last equations we omitted higher order corrections in μ_0. When $J_\perp \neq 7J_z$, Eq. (37) can be written in the canonical form

$$U_T + (\alpha U + 6U^2)U_X \pm U_{XXX} = 0 \tag{39}$$

after a scaling transformation. Parameter α that we introduced here is proportional to the deviation from half-filling, $\alpha \sim \mu_0$, and we assume it to be small.

Eq. (39) is called the modified Korteweg–de Vries (mKdV) equation and represents an integrable system as well as the KdV equation (see [90]). Let us note also that the mKdV equation is connected with the KdV equation by the Miura transformation [64] which was the first observation of the integrability properties of the KdV equation itself (see [69]).

There is a wider variety of soliton excitations that one can construct in the mKdV problem. At a fixed value of the chemical potential one can find both particle-like and hole-like solitons moving in the same direction. This should be contrasted to the situation away from half-filling, which we discussed in the previous section, where at a given chemical potential and direction of propagation we had either particle or hole like solitons, but never both simultaneously. For the mKdV case we also find soliton excitations which look like particle on a pedestal (or hole on a pedestal). We provide a detailed discussion of solitons in the mKdV problem and their manifestations for our system in the Appendix.

5.2. Close to integer filling. Nonlinear Schrödinger equation

When the system is close to integer filling $\mu_0 = \pm 1$. In this case characteristic velocities of the linearized system (19) coincide. Hence we can no longer assume separation of the left- and right-moving parts. Examining systems (29) and (30) we find that dispersive corrections also have singularities in variables (ρ, k).

To avoid these difficulties we return to variables (θ, σ), which we used before, and consider the Lagrangian density

$$\mathcal{L} = \frac{1}{2}\sigma_T \cos\theta - 2J_\perp \sin^2\theta \cos\sigma_X - 2J_z \cos^2\theta - h^2 J_\perp \sin\theta(\sin\theta)_{XX} \cos\sigma_X$$
$$- h^2 J_\perp \sin^2\theta\left(\frac{1}{6}\sigma_{XXX}\sin\sigma_X + \frac{1}{4}\sigma_{XX}^2\cos\sigma_X\right) - h^2 J_z \cos\theta(\cos\theta)_{XX} + \mathcal{O}(h^4) \tag{40}$$

in the limit $\theta \to 0, \pi$. If we keep only quadratic terms in $(\sin\theta, \sigma)$ in the dispersive part of the Lagrangian, we can write the corresponding equations of motion as (in the limit $\mu_0 = \pm 1$)

$$\sigma_T \sin\theta + 8J_\perp \sin\theta \cos\theta \cos\sigma_X - 8J_z \cos\theta \sin\theta + 4h^2 J_\perp \mu_0 (\sin\theta)_{XX} = 0$$
$$\theta_T - 8J_\perp (\sin\theta)_X \sin\sigma_X - 4J_\perp \sin\theta(\sin\sigma_X)_X = 0 \tag{41}$$

If we keep only the lowest order cubic terms in the nonlinear part of (41), we can rewrite this equation for small (θ, σ) as

$$\sigma_T \sin\theta + 8\mu_0(J_\perp - J_z)\sin\theta - 4\mu_0(J_\perp - J_z)\sin^3\theta - 4\mu_0 J_\perp \sin\theta\sigma_X^2 + 4h^2\mu_0 J_\perp(\sin\theta)_{XX} = 0$$

$$\theta_T - 8J_\perp(\sin\theta)_X \sigma_X - 4J_\perp \sin\theta\sigma_{XX} = 0$$

$(\mu_0 = \pm 1)$.

It is not difficult to verify that the system above can be written in the form of the defocusing nonlinear Schrödinger equation

$$ih\psi_T = 8(J_\perp - J_z)\psi - 4(J_\perp - J_z)|\psi|^2\psi + 4h^2 J_\perp\psi_{XX} \tag{42}$$

for the function

$$\psi = \sin\theta e^{i\mu_0\sigma/h} = \sin\theta e^{i\mu_0\varphi}$$

Eq. (42) describes an integrable system [97], which was solved by Zakharov and Shabat by the inverse scattering method. System (42) admits an exact description of the evolution starting from any initial state. However, nonlinear Schrödinger equation does not have soliton solutions in the defocusing case. Defocusing nature of Eq. (42) demonstrates stable behavior of the system with respect to initial perturbations. In this case asymptotic behavior of solutions of (42) should only include wave-trains which "dissolve" for $T \to \infty$ [96].[2]

5.3. Special filling factor

We now comment on the special point of our system at

$$\mu_0 = \sqrt{J_\perp - 7J_z}/\sqrt{7(J_\perp - J_z)} \tag{43}$$

for the case $0 < J_z < J_\perp/7$. To get Eqs. (33) and (34) from (31) and (32) we need to make scaling transformation

$$X \to X \bigg/ h\left(\frac{2(1-\mu_0^2)J_\perp}{J_\perp - J_z}\right)^{1/4}\left|J_\perp\left(\frac{1}{6} - \frac{\mu_0^2}{1-\mu_0^2}\right) - \frac{7}{6}J_z\right|^{1/2}$$

This transformation is singular at the special point (43). As a corollary, the width of solitons (and the period of oscillations in the "wave-train" part) become small in X-space w.r.t. another parameter

$$\mu_0 - \sqrt{J_\perp - 7J_z}/\sqrt{7(J_\perp - J_z)}$$

Higher dispersive terms become important in this limit and Lagrangian density (12) can no longer be used. As we discussed earlier, dynamics is more complicated near this special point, and one should use original lattice system (8) to discuss dynamics. In general we expect here oscillation zones with rather short period of oscillations.

---

[2] The soliton solutions on the "pedestal" are also possible for Eq. (42). We do not consider them here.

6. Decay of the density step

We now apply our general arguments to understand dynamical evolution starting from a specific initial state. We assume that at $T = 0$ we have a smooth step-like change in the density without any initial current. Experimentally such initial configuration can be created using a smooth step in the external potential that is suddenly removed. This initial state is of the form given by Eq. (18). It is shown schematically in Fig. 5. In this section we only consider the situation when the system is not close to any special points. Density step decay for systems close to half-filling is discussed in the Appendix.

Since we rely on the long wavelength expansion, we assume that function $\rho(X, T = 0)$ is a slow function of the spatial coordinate.

The main terms in the long wavelength expansion of dynamics are given by the wave Eq. (19). The wave equation predicts that after a short time the step-like initial state should turn into a two-step solution, with two steps propagating in the opposite directions (see Fig. 6). When the two steps separate from each other, they can be analyzed independently. The left- and right-moving edges of the solution correspond to r_1 and r_2. Proceeding to the next order in h, we find that they are described by Eqs. (31) and (32), respectively. After rescaling of coordinates (X, T) and functions r^1 and r^2 themselves, this dynamics is given either by Eq. (33) or (34), where the choice depends on the values of $(J_\perp, J_z, \text{and } \mu_0)$.

First of all, we need to understand whether hydrodynamic solutions for r_1 and r_2 break down and develop a singularity. For $\mu_0 > 0$ and the initial density profile shown in Fig. 5 the steepness of function $r^1(X)$ should increase with time while the steepness of function $r^2(X)$ should decrease with time (see Fig. 7). This follows from simple hydrodynamic analysis following Eqs. (26) and (27). This means that the steepness of solutions $\rho(X), k(X)$ will increase on the left-moving edge of Fig. 6 and decrease on the right-moving edge. (The situation changes to the opposite for the inverse step initial state.) So in this case no dispersive corrections are needed for $r^2(X)$. Function $r^2(X)$ should remain smooth for all $T > 0$ in
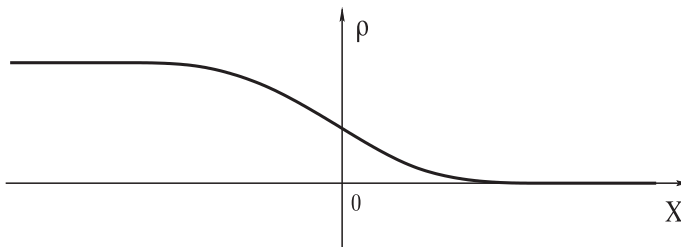

Fig. 5. The step-like initial conditions for the function $\rho(X,T)$ with the assumption $\varphi(X,0) = 0$.
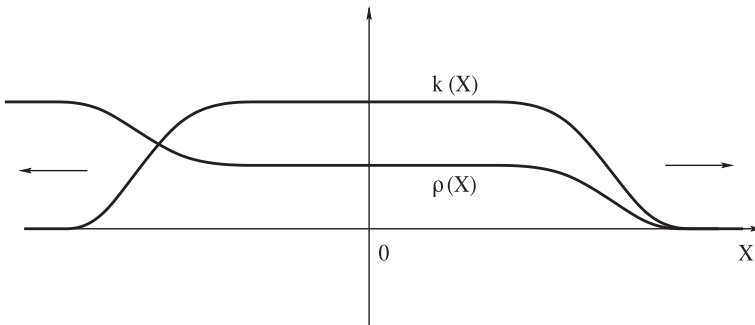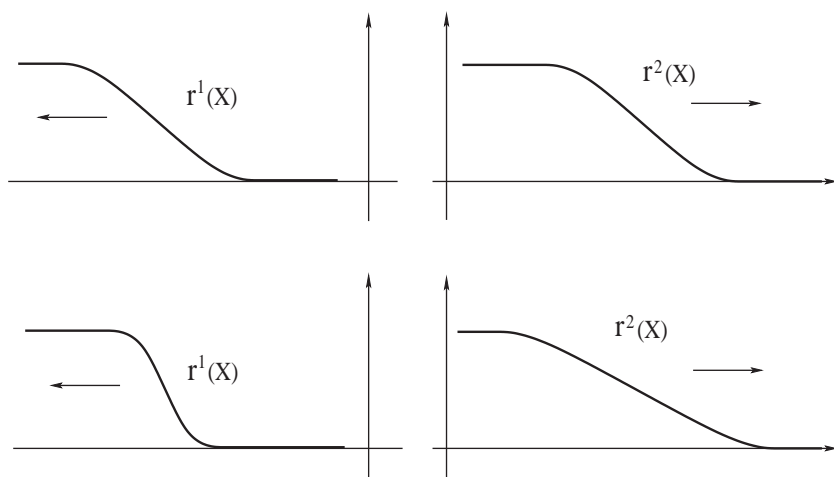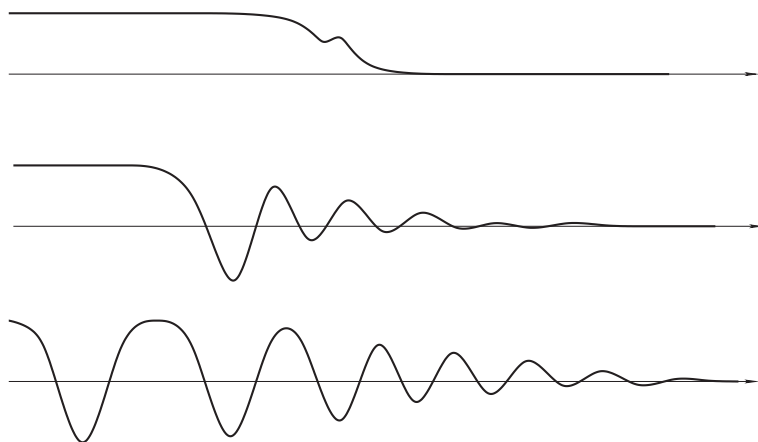

Fig. 6. The evolution of initial distribution with $k(X,0) = 0$ and the step-like $\rho(X,0)$ in the approximation of system (19).

Fig. 7. The increasing of the steepness of solution $r^1(X)$ on the left-moving edge and the decreasing of the steepness of solution $r^2(X)$ on the right-moving edge in the hydrodynamic approximation. The data are sketched in the original coordinate system.
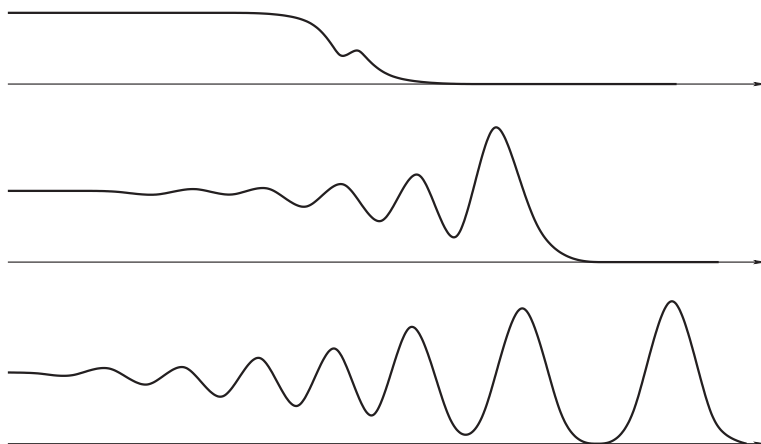

Fig. 8. The development of oscillation zone from the step-like initial data for the case of Eq. (33).

the hydrodynamic approximation. On the other hand, function $r^1(X)$ develops a breaking point in the hydrodynamic approximation. Thus we need to consider Eq. (31) taking into account dispersive corrections. As we discussed before dispersive corrections should give rise the oscillation zone, which we expect to grow linearly with time. The form of oscillations should be different for Eqs. (33) and (34) due to different signs of dispersion in these systems (see Figs. 8 and 9).

To understand the oscillation zone that arises following breaking of the hydrodynamic solution we need to analyze dynamics of the KdV equation with step like initial conditions. This problem was addressed by Gurevich and Pitaevskii [31,32] using the Whitham theory of slow modulations. We will now summarize their key results pointing out their implications for our system.

Gurevich and Pitaevskii considered a general problem of slowly modulated one-phase solution of the KdV equation. One-phase solution is a periodic running wave solution that provides a generalization of the one-soliton solutions of the KdV equation

Fig. 9. The development of oscillation zone from the step-like initial data for the case of Eq. (34).
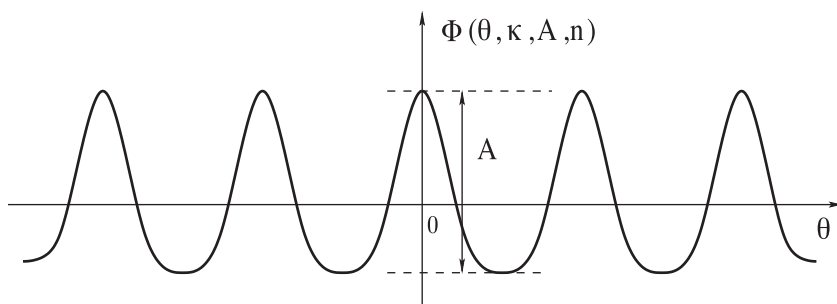
Fig. 10. The general form of the function $\Phi(\theta,\kappa,A,n)$ representing the one-phase solution of the KdV-equation.

$$U(X,T) = \Phi(\kappa X + \omega T + \theta_0, \kappa, A, n)$$

One-phase solution depends on three parameters (κ, A, n). Functions $\Phi(\theta, \kappa, A, n)$ should be 2π-periodic in θ, so parameter κ plays the role of the wave number for nonlinear running waves. Parameter A plays the role of the amplitude of the periodic solution, while parameter $n = \langle \Phi \rangle$ is the value of Φ averaged over one period (see Fig. 10).

One-phase solutions of KdV can be written in the form

$$\Phi(\kappa X + \omega T, \kappa, A, n) = \frac{A}{s^2} \mathrm{dn}^2 \left[\left(\frac{A}{12s^2} \right)^{1/2} (X - VT), s \right] + \gamma$$

$$V = \frac{A}{3s^2}(2 - s^2) + \gamma$$

where s is the modulus of the Jacobi elliptic function $\mathrm{dn}(u,s)$, $0 \leqslant s \leqslant 1$. The values (κ, ω, n) can be expressed in terms of the parameters (A, s, γ) in the following way

$$\kappa = \frac{\pi}{K(s)} \left(\frac{A}{12s^2} \right)^{1/2}, \quad \omega = -V\kappa = -\frac{4\pi}{K(s)}(2 - s^2) \left(\frac{A}{12s^2} \right)^{3/2} - \frac{\gamma\pi}{K(s)} \left(\frac{A}{12s^2} \right)^{1/2}$$

$$n = \gamma + \frac{AE(s)}{s^2 K(s)}$$

where $K(s)$ and $E(s)$ are the elliptic integrals of the first and the second kind respectively.

We can also write

$$\Phi(\theta, A, s, \gamma) = \frac{A}{s^2} \mathrm{dn}^2 \left(\frac{K(s)}{\pi} \theta, s \right) + \gamma$$

as normalization of function $\Phi(\theta, \kappa, A, n)$.

The one-soliton solutions of KdV can be considered as the limiting case of the one-phase solutions in the large-period limit $\kappa \to 0$. Traditionally the asymptotes $\Phi(\theta) \to 0$, $\theta \to \pm\infty$ is assumed for the soliton solutions of KdV, so the amplitude parameter A remains the one parameter of a one-soliton solution.

In Whitham's approach parameters (κ, A, n) become slow functions of x and t

$$\kappa = \kappa(X, T), \quad A = A(X, T), \quad n = n(X, T)$$

so that functions $\kappa(X,T)$, $A(X,T)$, $n(X,T)$ satisfy a nontrivial system of quasilinear equations in partial derivatives (the so-called Whitham's system). Whitham's system describes evolution of initial parameters $\kappa(X,0)$, $A(X,0)$, $n(X,0)$ of oscillating solutions, such that development of oscillations can be calculated in this case.

Gurevich and Pitaevskii showed that in the KdV equation with a step like initial conditions, the small oscillation zone, that arises near the breaking point of the hydrodynamic solution, can be described by the self-similar solutions characterized by only one variable, $l = X/T$.

In more details, the asymptotic $(T \to \infty)$ form of oscillations can be described by the modulated one-phase solutions of KdV with parameters $\kappa(X,,T)$, $A(X,T)$, $n(X,T)$ of the form

$$\kappa(X, T) = \kappa(X/T), \quad A(X, T) = A(X/T), \quad n(X, T) = n(X/T)$$

The oscillation zone is located in the interval

$$l_- < X/T < l_+$$

in this asymptotic regime.

According to [31,32] the amplitude of oscillations $A(X,T)$ becomes zero at the "trailing edge" of the oscillation zone (the right edge in Fig. 8 and the left edge in Fig. 9). The wave number of nonlinear oscillations $\kappa(X,T)$ becomes zero at the "leading edge" of the oscillation zone (the left edge in Fig. 8 and the right edge in Fig. 8).

We can see that the "trailing edge" of oscillation zone can be considered as a source of oscillations with small amplitude, which develop into solitons in the limit $T \to \infty$. The "leading edge" of the oscillation zone can be considered as a source of free solitons since we have $\kappa \to 0$ on this edge and the distance between solitons tends to infinity for $T \to \infty$.

We point out that it is also possible to analyze the problem above in terms of the "pure" soliton picture [58,59]. Approach used in [58,59] is also a classical part of the soliton theory.

General problem of the decay of different initial configurations in the theory of small-dispersion KdV-equation represents a big branch of the soliton theory. While we do not discuss other problems here, we expect that many of the known mathematical results will be relevant for different experiments with ultracold atoms. We also point out that our methodology for identifying the character of solitons (particle- or hole-like) was based on considering the function $U(X,T)$, which describes Riemann invariants $r^1(X,T)$ or $r^2(X,T)$. It is more natural to classify solitons based on the density. Relations between $r^{\{1,2\}}(X,T)$ and the more physical variables of the density, $\rho(X,T)$, and the phase gradient, $k(X,T)$, are given in Eq. (24). We find that the density always follows the behavior of $r^{\{1,2\}}(X,T)$. Hence our classification of the hole-type and the particle-type solitons in terms of the density coincides with that given in terms of the function $U(X,T)$.

Before concluding this section we would like to point out that whether step-like conditions shown in Fig. 5 should be considered as a source of hole-like or particle-like solitons in the solutions $\rho(X,T)$, $k(X,T)$ depends on the relation between parameters $(J_\perp, J_z, \mu_0)$. In general, we expect that larger values of J_z and μ_0 suppress the appearance of hole-type solitons and favor solitons of the particle type. On the opposite side, smaller values of J_z and μ_0 allow solitons of the hole type and suppress solitons of particle type.

7. Two-dimensional effects

In this section we discuss the role of transverse directions. We consider a question of whether one dimensional profiles, that we discussed so far, are stable against "weak" modulation in the transverse direction.

For a D-dimensional lattice we need to change the long wavelength Lagrangian density (40) to a more general expression

$$
\mathcal{L} = \frac{1}{2}\sigma_T \cos\theta - 2J_\perp \sin^2\theta \sum_{i=1}^{D} \cos\sigma_{X^i} - 2J_z D \cos^2\theta
$$

$$
- h^2 J_\perp \sin\theta \sum_{i=1}^{D} (\sin\theta)_{X^i X^i} \cos\sigma_{X^i} - h^2 J_z \cos\theta \sum_{i=1}^{D} (\cos\theta)_{X^i X^i}
$$

$$
- h^2 J_\perp \sin^2\theta \sum_{i=1}^{D} \left(\frac{1}{6}\sigma_{X^i X^i X^i} \sin\sigma_{X^i} + \frac{1}{4}\sigma_{X^i X^i}^2 \cos\sigma_{X^i} \right) + \mathcal{O}(h^4)
$$

or

$$
\mathcal{L} = \frac{1}{2}\sigma_T \mu - 2J_\perp (1-\mu^2) \sum_{i=1}^{D} \cos\sigma_{X^i} - 2J_z D \mu^2
$$

$$
+ h^2 J_\perp \frac{\mu^2}{1-\mu^2} \sum_{i=1}^{D} \mu_{X^i}^2 \cos\sigma_{X^i} - h^2 J_z \mu \sum_{i=1}^{D} \mu_{X^i X^i}
$$

$$
+ h^2 J_\perp (1-\mu^2) \sum_{i=1}^{D} \left(\frac{1}{3}\sigma_{X^i X^i X^i} \sin\sigma_{X^i} + \frac{1}{4}\sigma_{X^i X^i}^2 \cos\sigma_{X^i} \right) + \mathcal{O}(h^4)
$$

in the coordinates (μ, σ).

We separate the hydrodynamic and dispersive parts of the Lagrangian and repeat considerations used in the previous sections. Analysis of the dynamical system is more complicated for $D > 1$ and we will not explore all of its richness. We only address a question whether one dimensional solitons that we discussed so far are stable with respect to formation of a two dimensional pattern (see Fig. 11).

We start with a generic situation corresponding to Eq. (33) or (34). Since we are going to consider only small modulations of the soliton strings, we can follow the procedure suggested in [43] to get the Kadomtsev–Petviashvili equation for two-dimensional systems.
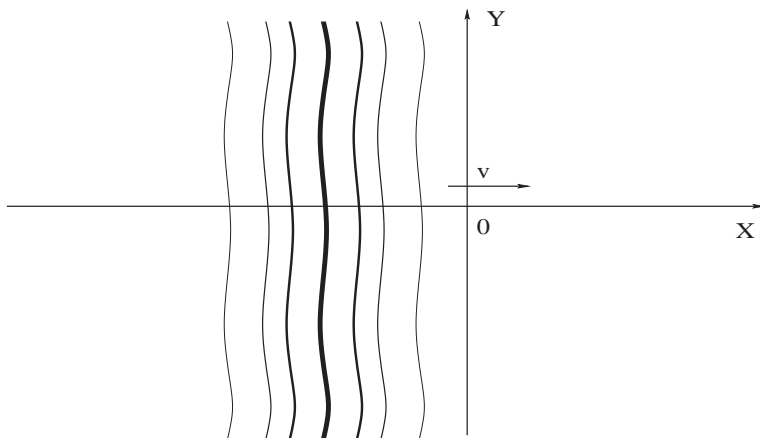

Fig. 11. Schematic sketch of a one-dimensional soliton string modulated in the *Y*-direction.

Firstly we recall that Eqs. (31)-(32) are written in the moving coordinate systems. For the left-moving part of the solution in the laboratory frame of reference we have

$$r_T^1 = \sqrt{J_\perp(J_\perp - J_z)}\sqrt{32(1 - \mu_0^2)}r_X^1 - 6\mu_0\sqrt{J_\perp(J_\perp - J_z)}r^1 r_X^1$$
$$+ \sqrt{2}h^2\sqrt{1 - \mu_0^2}\sqrt{\frac{J_\perp}{J_\perp - J_z}}\left(J_\perp\left(\frac{1}{6} - \frac{\mu_0^2}{1 - \mu_0^2}\right) - \frac{7}{6}J_z\right)r_{XXX}^1 \tag{44}$$

In writing the last equation we preserved the restriction $r^2 = const$.

The first term in the right-hand part plays the main role in the evolution of $r^1(X, T)$ and other terms represent small corrections with respect to the main contribution. According to [43] we only need to calculate corrections to the main term coming from the slow modulation of the solution in the Y-direction. This procedure gives us stable or unstable variants of the Kadomtsev–Petviashvili equation. The main term in the right-hand part of (44) originates from the linear system (19) of (20) which can be easily written in the two-dimensional form by adding additional derivatives in the Y-direction. What we need here is correction to the dispersion law $\omega^2 \sim k_X^2$ which can be written as

$$\omega = v_0\sqrt{k_X^2 + k_Y^2} \sim \sqrt{J_\perp(J_\perp - J_z)}\sqrt{32(1 - \mu_0^2)}\left(k_X + \frac{1}{2}\frac{k_Y^2}{k_X}\right)$$

for the left-moving part in our situation.[3] As a result, the small modulations in the Y-direction of solutions of (44) can be described by the equation

$$r_{TX}^1 = \sqrt{J_\perp(J_\perp - J_z)}\sqrt{32(1 - \mu_0^2)}r_{XX}^1 - 6\mu_0\sqrt{J_\perp(J_\perp - J_z)}(r^1 r_X^1)_X$$
$$+ \sqrt{2}h^2\sqrt{1 - \mu_0^2}\sqrt{\frac{J_\perp}{J_\perp - J_z}}\left(J_\perp\left(\frac{1}{6} - \frac{\mu_0^2}{1 - \mu_0^2}\right) - \frac{7}{6}J_z\right)r_{XXXX}^1$$
$$+ \frac{1}{2}\sqrt{J_\perp(J_\perp - J_z)}\sqrt{32(1 - \mu_0^2)}r_{YY}^1$$

or

$$r_{TX}^1 = \frac{1}{2}\sqrt{J_\perp(J_\perp - J_z)}\sqrt{32(1 - \mu_0^2)}r_{YY}^1 - 6\mu_0\sqrt{J_\perp(J_\perp - J_z)}(r^1 r_X^1)_X$$
$$+ \sqrt{2}h^2\sqrt{1 - \mu_0^2}\sqrt{\frac{J_\perp}{J_\perp - J_z}}\left(J_\perp\left(\frac{1}{6} - \frac{\mu_0^2}{1 - \mu_0^2}\right) - \frac{7}{6}J_z\right)r_{XXXX}^1 \tag{45}$$

in the moving coordinate system.

Eq. (45) is the Kadomtsev–Petviashvili (KP) equation which describes the small transverse modulations of solutions of the KdV equation considered in the two-dimensional case. The stable Kadomtsev–Petviashvili equation corresponds to the same signs of the coefficients for r_{XXXX}^1 and r_{YY}^1. In this case the small modulation of a soliton string causes just the weak oscillations along the string and does not produce any instability. The opposite situation with different signs of the coefficients before r_{XXXX}^1 and r_{YY}^1 corresponds to the unstable situation where the soliton strings are unstable with respect to modulation along the Y-axis.

We can see then that the stable soliton string in two dimensions arises for the situation of Eq. (33), i.e.

$$J_z < J_\perp/7, \quad -\sqrt{\frac{J_\perp - 7J_z}{7(J_\perp - J_z)}} < \mu_0 < \sqrt{\frac{J_\perp - 7J_z}{7(J_\perp - J_z)}}$$

which corresponds to the small values of J_z and the density $n \sim 1/2$ in the pattern.

The solutions we considered in the opposite situation

---

[3] We use the expansion of the solutions of linear system in the form $f(X, T) = \int f(\mathbf{k})e^{i\omega(\mathbf{k})T + i\mathbf{kR}}d\mathbf{k}$.

$$J_z > J_\perp/7 \quad \text{or} \quad |\mu_0| > \sqrt{\frac{J_\perp - 7J_z}{7(J_\perp - J_z)}}$$

are unstable from the point of view of the two-dimensional modulations.[4]

Let us say now that the analogous considerations can be performed also in the case of Eq. (39) so the results formulated above can be used also in the limit $\mu_0 \to 0$.

We must certainly say that the Kadomtsev–Petviashvili equation is an integrable system from the point of view of the inverse scattering methods [19,98]. The theory of Eq. (45) is very deep and brought many beautiful ideas in the theory of solitons. Let us just mention here two nice classes of solutions of (45) in the stable and the unstable situation.

(1) The most interesting solutions of the Kadomtsev–Petviashvili equation in the stable situation are the two-dimensional N-soliton solutions which are described in general by the formula

$$U(X, Y, T) = \Phi\left(\omega^1 T + k_X^1 X + k_Y^1 Y + c^1, \ldots, \omega^N T + k_X^N X + k_Y^N Y + c^N\right)$$

with some special functions $\Phi(\theta^1, \ldots, \theta^N)$ [78].
The N-solution solutions of the KP equation represent N plane interacting waves propagating at some angles with respect to each other. The interaction of the waves results in the phase shifts which can be rather big in the resonant case [63].

(2) For the unstable variant of the KP equation very interesting rational localized solutions ("lumps") can arise. The "lumps" represent localized both in X- and Y-direction solitons with rational dependence of coordinates. The interaction of solitons does not produce any phase shifts in this situation, so the solitons completely "forget" about each other after the interaction [10].

Let us emphasize here that the relation $J_\perp > J_z$ was assumed everywhere in our considerations above and the properties we consider will be completely changed for the opposite situation $J_\perp < J_z$. Thus, as we pointed out already, the hydrodynamic approximation (15) reveals an elliptic instability for the small values of $k(k < \pi/2)$ in this situation which corresponds to a modulation instability of long-wave solutions of (8) in this case. In the same way, Eq. (42) becomes the focusing nonlinear Schrödinger equation in this situation which corresponds to the unstable behavior of the long-wave solutions of (8) either. However, the integrable nature of the focusing nonlinear Schrödinger equation leads to very interesting behavior of solutions also in this case. The most interesting part is the presence of the N-soliton solutions for the focusing NLS equation which should be observed for $J_z > J_\perp$. The corresponding two-dimensional equation for (42) can be written in the form

$$ih\psi_T = 8(J_\perp - J_z)\psi - 4(J_\perp - J_z)|\psi|^2\psi + 4h^2 J_\perp \psi_{XX} + 4h^2 J_\perp \psi_{YY} \qquad (46)$$

The one-dimensional solutions of (46), however, are unstable with respect to the weak transverse modulations [6] for $J_z > J_\perp$.

8. Concluding remarks

Soliton solutions in quantum systems is a subject of considerable theoretical interest. However, most of the earlier work focused on one dimensional systems, where special analytical tools, such as the Bethe ansatz solution, are available. For example, exact solitonic solutions were considered recently in a different quantum system in a series of papers [7–9]. Their analysis relied on the quantum inverse scattering methods, which are special to 1d integrable systems. Our analysis in this paper is on constructing semiclassical solitons in two and three dimensional systems.

States described by the wavefunction (5) correspond to collective excitations in the superfluid state. In the superfluid state the U(1) symmetry is spontaneously broken, so the number of particles

---

[4] Let us note here that these conclusions do not require in fact the square two-dimensional lattice and are applicable for any dispersion law $\omega^2 = \alpha k_X^2 + \beta k_Y^2$, $\alpha, \beta > 0$ in the main linear approximation.

is not a good quantum number. Solitons which we discuss in this papers are semiclassical collective excitations. They can be thought of as spatially inhomogeneous coherent states representing non-linear excitations of the Hamiltonian. These solitons do not have a well defined number of particles. Within our approximations solitons have infinite lifetime. We expect that including coupling to other excitations may give rise to small but finite decay rate for the solitons, which may lead to dissipative terms in the semiclassical dynamics. We expect that this should not change our conclusions qualitatively, since solitons should be robust against small dissipation [67].

Acknowledgments

Appendix A

A.1. General approach for analyzing solitonic solutions in KdV-type equations

The famous procedure of integration of the KdV equation [27] is based on the connection of the KdV with the linear Schrödinger operator passing through the iso-spectral deformations according to the KdV evolution. The corresponding linear problems have the form

$$-\psi_{XX} + U\psi = E\psi \tag{47}$$

for Eq. (33), and

$$-\psi_{XX} - U\psi = E\psi \tag{48}$$

for Eq. (34). The connection of the KdV equations with the linear problems (47) and (48) gives a possibility to represent also Eqs. (33) and (34) in the equivalent form [57]:

$$\frac{\partial}{\partial T}\widehat{L} = \widehat{L}\widehat{A} - \widehat{A}\widehat{L} \tag{49}$$

where the operators $\widehat{L}, \widehat{A}$ have the form

$$\widehat{L} = -\frac{d^2}{dX^2} + U, \quad \widehat{A} = -4\frac{d^3}{dX^3} + 6U\frac{d}{dX} + 3U_X$$

for Eq. (33) and

$$\widehat{L} = -\frac{d^2}{dX^2} - U, \quad \widehat{A} = 4\frac{d^3}{dX^3} + 6U\frac{d}{dX} + 3U_X$$

for Eq. (34). Representation (49) of the KdV equation permits to consider the KdV evolution as the iso-spectral deformation of the operator $\widehat{L}$ using the exponent of the operator $\widehat{A}$ as the corresponding basis transformation.

According to the procedure represented in [27] the scattering problem for the linear Eqs. (47) and (48) plays the basic role in solving Eqs. (33) and (34) in the rapidly decreasing case $|U(X)| \to 0, X \to \pm\infty$. Thus, if we consider the eigen-functions of (47) or (48) having the asymptotic form

$$\psi(X) \simeq e^{ikX} + b(k)e^{-ikX}, \quad X \to -\infty, \quad \psi(X) \simeq a(k)e^{ikX}, \quad X \to \infty$$

$(k^2 = E)$ and introduce the reflection and transition coefficients $r(k), t(k)$ in the standard way we will have very simple evolution of the functions $r(k,T), t(k,T)$:

$$t(k,T) = t(k,0), \quad r(k,T) = e^{\pm 8ik^3 T} r(k,0)$$

according to the KdV evolution of $U(X,T)$.[5]

In the same way, if the potential $U(X)$ has bounded states $\psi_n(X)$ with the energies E_n we will have $E_n = const$ during all the KdV evolution. From the other hand, provided that the functions $\psi_n(X)$ are normalized in the following way

$$\psi_n(X) \simeq e^{k_n X}, \quad X \to -\infty, \quad \psi_n(X) \simeq C_n e^{-k_n X}, \quad X \to \infty$$

$(-k_n^2 = E_n)$ the evolution of the values $C_n(T)$ is given by $C_n(T) = e^{\pm 8k_n^3 T} C_n(0)$.

The full set of the scattering data

$$\{r(k), E_n, C_n\}$$

gives the full information about the potential $U(X)$ [25,61,45] such that the solution $U(X,T)$ can be reconstructed at every time T using the values of $r(k,T)$, E_n, $C_n(T)$.

The potentials $U(X)$ having zero reflection coefficient $r(k) \equiv 0$ are called the reflectionless potentials and correspond to the exact N-soliton solutions of the KdV-equation. The number of the bounded states $(n = 1, \ldots, N)$ is equal to the number of solitons in the N-soliton solution, so we can say that every bounded state in potential $U(X)$ corresponds to a soliton in the solution $U(X,T)$. The one-soliton solutions of the KdV-equation have the form

$$U(X,T) = -\frac{2a^2}{\text{ch}^2(aX + 4a^3 T + c_0)} \tag{50}$$

for Eq. (33) and

$$U(X,T) = \frac{2a^2}{\text{ch}^2(aX - 4a^3 T + c_0)} \tag{51}$$

for Eq. (34). Potentials (50) and (51) have exactly one bounded state according to linear problems (47) and (48), respectively with energy $E_1 = E_1(a)$ depending on the amplitude of a soliton.

A.2. Analysis of solitons close to half-filling. Modified KdV equation

In this section we discuss soliton solutions of two types of the mKdV equations:

$$U_T + 6U^2 U_X - U_{XXX} = 0 \tag{52}$$
$$U_T + 6U^2 U_X + U_{XXX} = 0 \tag{53}$$

(we put $\alpha = 0$ here).

Eq. (53) has two varieties of one-soliton solutions of arbitrary amplitude defined by the analytic formula

$$\pm \int \frac{dU}{\sqrt{vU^2 - U^4}} = X + C$$

Here U should be taken from one of the regions in the U-space where the value of expression $vU^2 - U^4$ is positive (see Fig. 12).

It is then easy to see that we can have either the particle-type or hole-type solitons, both moving to the right $(v > 0)$[6] and connected by the transformation $U \to -U$ (Fig. 13).

Soliton velocity is proportional to the square of the amplitude $v \sim A^2$ and we can have arbitrary positive value of A. Explicit formula for the one-soliton solutions of (53) can be written in the form

$$U = \pm \frac{a}{\text{ch}(aX - a^3 T + c_0)}$$

[5] We have different signs in the evolution of r for Eqs. (33) and (34).

[6] We remind the readers that this analysis is done in the left-moving coordinate system. Velocity of solitons with respect to the moving frame should be much smaller than the velocity of the reference frame moving.
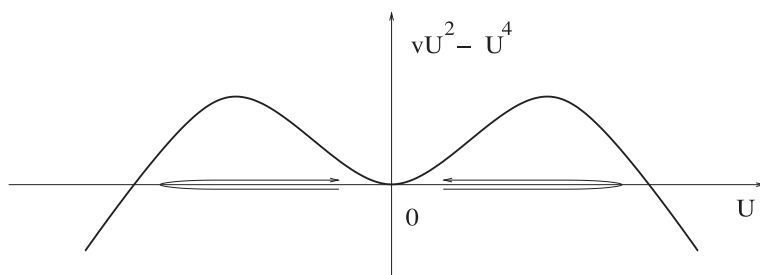
Fig. 12. The left and right paths of integration w.r.t. U corresponding to hole- and particle-type one-soliton solutions of (53).
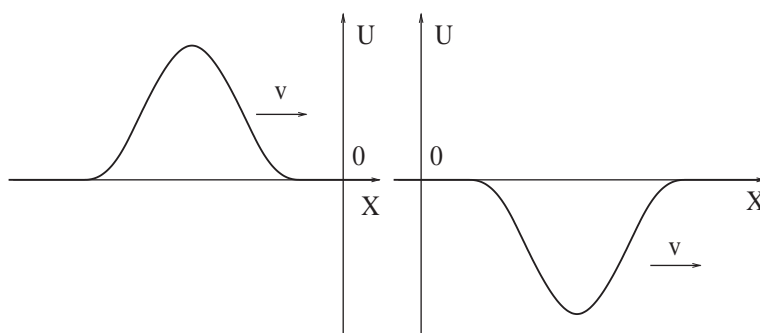
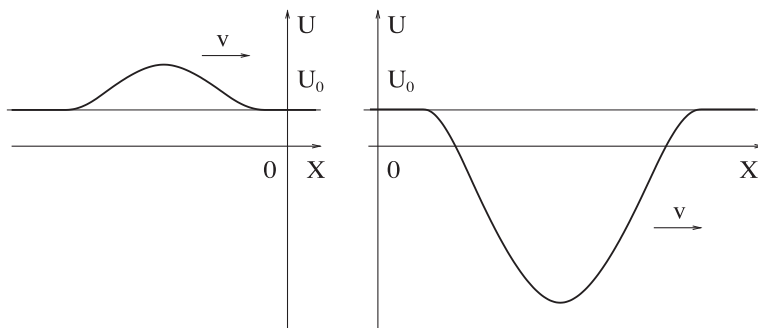**Fig. 13.** The particle- and the hole-type solitons for Eq. (53).
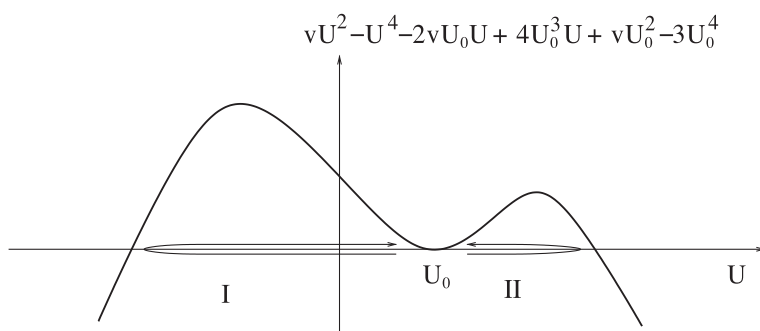
Fig. 14. The left and right paths of integration w.r.t. U corresponding to the hole- and t particle-type soliton solutions on a "pedestal" U_0 for (53).

Eq. (53) also admits more general soliton solutions. One can construct soliton solutions on a "pedestal". These solutions are defined by a more general analytic formula

$$\pm \int \frac{dU}{\sqrt{vU^2 - U^4 - 2vU_0U + 4U_0^3U + vU_0^2 - 3U_0^4}} = X + C$$

where two different paths of integration w.r.t. U are shown at Fig. 14.

Again we can have solitons of the particle and hole type, both on a "pedestal" $U = U_0$ moving with the speed v (our discussion is done in the moving frame) which can be represented by the following explicit formulas

Fig. 15. Solitons of the particle- and hole-type on the "pedestal" $U = U_0 > 0$ moving with the same velocity v for Eq. (53).

$$U = U_0 + \frac{a^2}{\sqrt{4U_0^2 + a^2}\,\text{ch}(aX - (6U_0^2 a + a^3)T + c_0) + 2U_0}$$

$$U = U_0 - \frac{a^2}{\sqrt{4U_0^2 + a^2}\,\text{ch}(aX - (6U_0^2 a + a^3)T + c_0) - 2U_0}$$

We have here $v = 6U_0^2 + a^2$ while the amplitudes of the particle-type and the hole-type solitons are given by the formulas

$$A_{p.t.} = \frac{a^2}{\sqrt{4U_0^2 + a^2} + 2U_0}, \quad A_{h.t.} = \frac{a^2}{\sqrt{4U_0^2 + a^2} - 2U_0}$$

(see Fig. 15).

We can now see the difference in the particle- and hole-type solitons in this new situation. For $U_0 > 0$ the amplitude of a particle type soliton can be arbitrarily small for $a \to 0$, while the amplitude of the hole-type soliton is bounded from below by the value $4U_0$ (the situation is opposite for $U_0 < 0$). We also see that solutions, which we consider, can be described as ordinary solitons of equation

$$U_T + \left(6U_0^2 + 12U_0 U + 6U^2\right)U_X + U_{XXX} = 0$$

after the shift $U \to U - U_0$. This coincides with the general mKdV Eq. (39) after a Galilean transformation.

We can claim then that regimes described by Eq. (34) (i.e. $J_\perp < 7J_z$, or $\mu_0^2 > (J_\perp - 7J_z)/7(J_\perp - J_z)$ if $J_\perp > 7J_z$) admit hole-type solitons after including the next nonlinear corrections. However, the small amplitude limit $A \to 0$ is possible only for $\mu_0 \to 0$ for the hole-type solutions. As a result, we expect that new solutions, which we discussed above, can only be observed when

$$J_\perp < 7J_z, \quad \mu_0 \to 0$$

and where changing from (34)–(53) is quite natural. In the regime

$$\mu_0^2 > (J_\perp - 7J_z)/7(J_\perp - J_z)$$

it is easy to see that the limit $\mu_0 \to 0$ is possible only for $J_\perp \sim 7J_z$. However, as we pointed out already, this situation is more complicated and should not be considered from the point of view of Eqs. (34) or (53). Thus, we can see that hole-type solitons can arise in the regimes corresponding to Eq. (34) for the situation $J_\perp < 7J_z$ in the limit $\mu_0 \to +0$ as a "reminiscent" of the region $\mu_0 < 0$ as follows from the higher corrections to (34).

The N-soliton solutions of Eq. (53) as well as the solution of the initial value problem can be constructed in the form analogous to the case of KdV (see [62,90]).

We can see then that Eq. (53) gives a good limiting case of Eq. (34) for $\mu_0 \to 0$ in the situation $J_\perp < 7J_z$. Moreover, Eq. (53) provides a good limit for both cases $\mu_0 > 0$ and $\mu_0 < 0$. The most remarkable feature of this regime is that both particle- and hole-type solitons with small amplitudes can coexist. The cubic nonlinear correction preserves the property of integrability of the corresponding evolution. Hence we expect that our analysis is applicable in the vicinity of the point $\mu_0 = 0$.

Let us turn now to the regimes described by Eq. (33) (i.e. $\mu_0^2 < (J_\perp - 7J_z)/7(J_\perp - J_z), J_\perp > 7J_z$) which correspond to Eq. (52) for $\mu_0 = 0$.

It is not difficult to see that Eq. (52) does not have real soliton solutions in ordinary sense and only the soliton solutions on "pedestal" can exist in this case. The one-soliton solutions on "pedestal" are defined by the analytic formula

$$\pm \int \frac{dU}{\sqrt{-\nu U^2 + U^4 + 2\nu U_0 U - 4U_0^3 U - \nu U_0^2 + 3U_0^4}} = X + C$$

where the path of integration w.r.t. U is shown in Fig. 16.

Explicit formula for the soliton solution can be written in the form

$$U = \pm \left[U_0 - \frac{2a^2}{\sqrt{U_0^2 - a^2}\,\text{ch}(2aX - (12U_0^2 a - 8a^3)T + c_0) + U_0} \right]$$

such that the soliton is of the hole-type for the positive "pedestal" and is of the particle-type for the negative pedestal ($U_0 > 0$) (Fig. 17).

The amplitude of soliton

$$A = \frac{2a^2}{\sqrt{U_0^2 - a^2} + U_0}$$

does not exceed the value $2U_0$ and can be arbitrarily small for $a \to 0$. The inverse scattering method and construction of the N-soliton solutions on "pedestal" for Eq. (52) were considered in [77] and Eq. (52) demonstrates that integrable properties are analogous to those of the KdV equation.

We can see then that Eq. (52) gives a satisfactory limit of the regimes described by Eq. (33) ($\mu_0^2 < (J_\perp - 7J_z)/7(J_\perp - J_z), J_\perp > 7J_z$) in the limit $\mu_0 \to 0$. We have to note, however, that the amplitude of solitons is restricted now by the value $2\mu_0$ for $\mu_0 \to 0$ and soliton solutions disappear for $\mu_0 = 0$. Thus, generation of solitons in the regimes corresponding to Eqs. (33) and (52) should be suppressed in the limit $\mu_0 \to 0$. This should be contrasted to the regimes corresponding to Eqs. (34) and (53).

A.3. Appendix. Step decay close to half-filling

One can use the inverse scattering method to solve initial value problems with localized initial perturbations for Eqs. (52) or (53) very similarly to what we discussed for Eqs. (33) or (34). However,
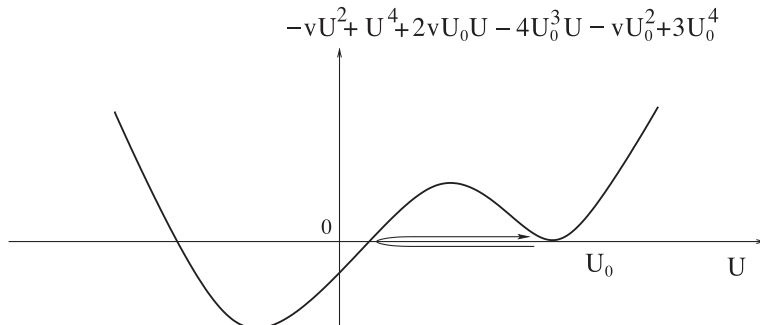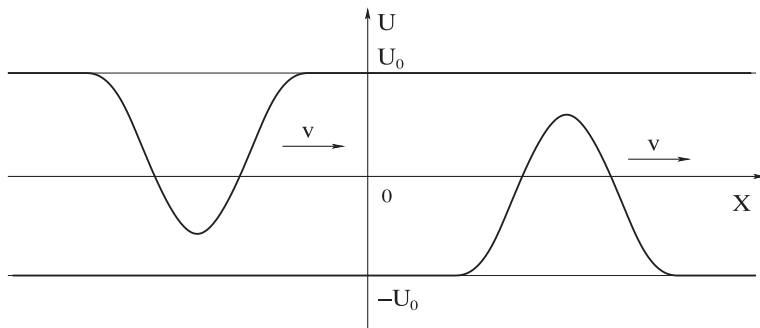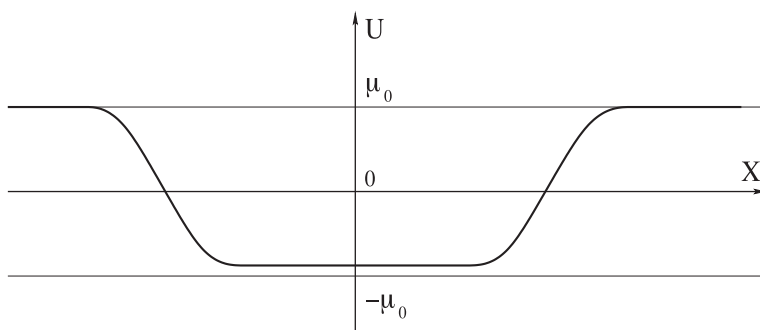
$$-\nu U^2 + U^4 + 2\nu U_0 U - 4U_0^3 U - \nu U_0^2 + 3U_0^4$$

Fig. 16. The path of integration w.r.t. U corresponding to a one-soliton solution on a "pedestal" for Eq. (52).

Fig. 17. The solitons of the hole type and of the particle type on the positive and negative "pedestals" for Eq. (52).

Fig. 18. The limiting form of a soliton solution for Eq. (52).

localized initial perturbation ($U(X) \to 0, X \to \pm\infty$) will be a source of solitons at final stages only for Eq. (53) for $\mu_0 = 0$. The soliton part will be absent in the solutions of (52). We also point out that for small $\mu_0 \neq 0$ and big amplitude of initial perturbation for Eq. (52) ($V_0 \gg \mu_0$) the "limiting" soliton (Fig. 18) in the limit $T \to \infty$ can arise [73].

We also discuss briefly dynamics starting from the step-like initial state for Eqs. (52) and (53) and the asymptotes of the corresponding solutions for $T \to \infty$. According to the type of the solutions we considered above we will consider now the initial data such that

$$U(X) \to U_1, \quad X \to -\infty, \quad U(X) \to U_2, \quad X \to +\infty$$

where both U_1 and U_2 are supposed to be small.

Let us note first of all that the situation here is not pretty much different from those shown at Figs. 8 and 9 in the case when U_1 and U_2 have the same signs (say $U_1, U_2 > 0$). So, the new features will arise here only in the case of different signs of U_1 and U_2 both for Eqs. (52) and (53).

Let us start again with Eq. (53).

We have to say first that the oscillation region arises now for the both kinds of steps for the different signs of U_1 and U_2 (see Fig. 19) and the situation with just a decreasing of the steepness of initial data shown at Fig. 7 is impossible in this case.

Both the situations shown at Fig. 19 for (53) result in the generation of solitons on the final stage which have the particle type in the first and the hole type in the second situation (Fig. 20).

We can see that the regimes of decay of step-like initial data for (53) include both the regimes coming from $\mu_0 > 0$ and $\mu_0 < 0$ which is rather natural and gives a good limit for $\mu_0 \to 0$.

Let us consider now the situation of Eq. (52) corresponding to the small values of J_z and μ_0. Let us consider the initial data shown at the top of Fig. 19 and suppose first that $|U_1| > |U_2|$. At the situation
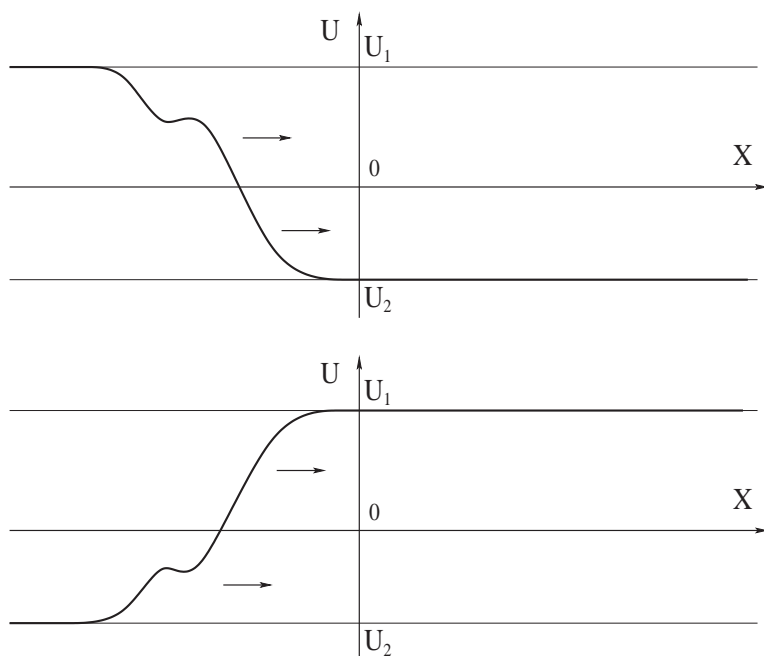
Fig. 19. Appearance of oscillations for two different kinds of steps for Eq. (39) in the case of different signs of U_1 and U_2.
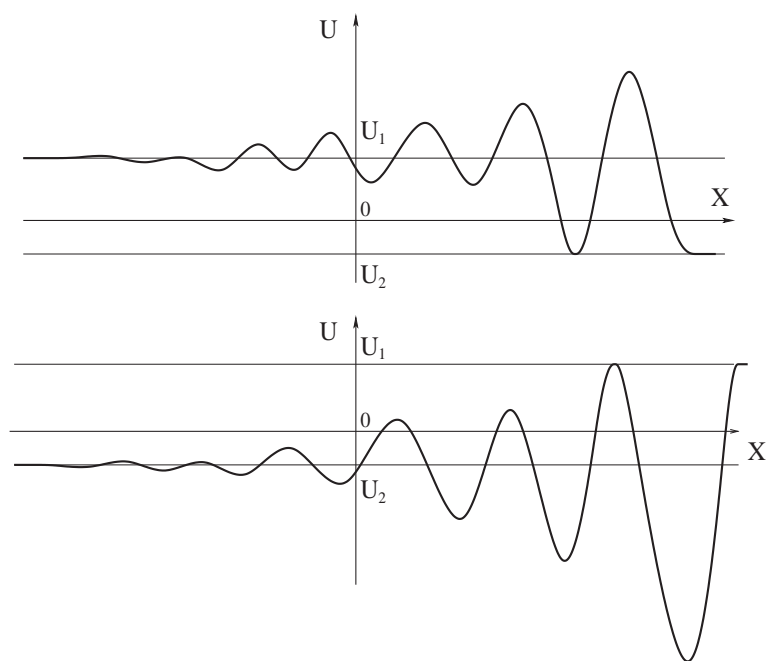
Fig. 20. The particle-type and hole-type solitons on the pedestals, U_1 and U_2, arising for two types of the step-like initial data for Eq. (53).

we describe the final stage of the oscillations development looks rather similar to that shown at Fig. 8 which is rather natural for the limit $\mu_0 \to 0$ in the pattern. However, the limit $|U_2| \to |U_1|$ demonstrates quite new features here which are connected with the arising of a new solution for Eq. (52). Indeed, for $|U_2| \to |U_1|$ the solitons arising in the decay of the step-like initial data have a "limiting" form (Fig. 18) which is connected with the separation of the "shock-wave" solution

$$U = -a\,\text{th}(aX - 2a^3T + c_0) \tag{54}$$

for $|U_2| = |U_1| = a$.

Solution (54) plays an important role in the decay of the step-like initial data we consider for (52) for $|U_2| \geqslant |U_1|$. Let us say that for general initial data having the form
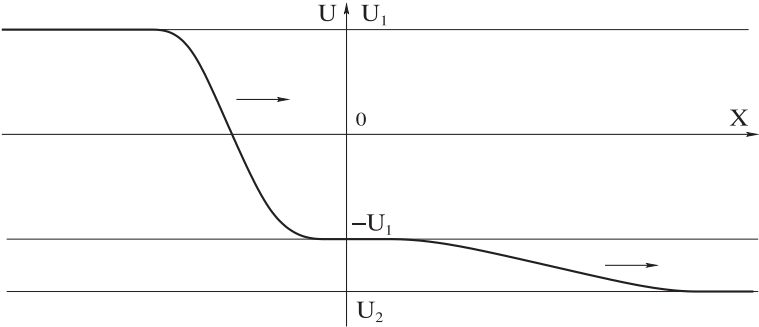
$$U(-\infty) = -U(+\infty) = a$$

Fig. 21. Additional step with decreasing steepness ($T \to \infty$) arising after the separation of solution (54) for $|U_2| > |U_1|$.
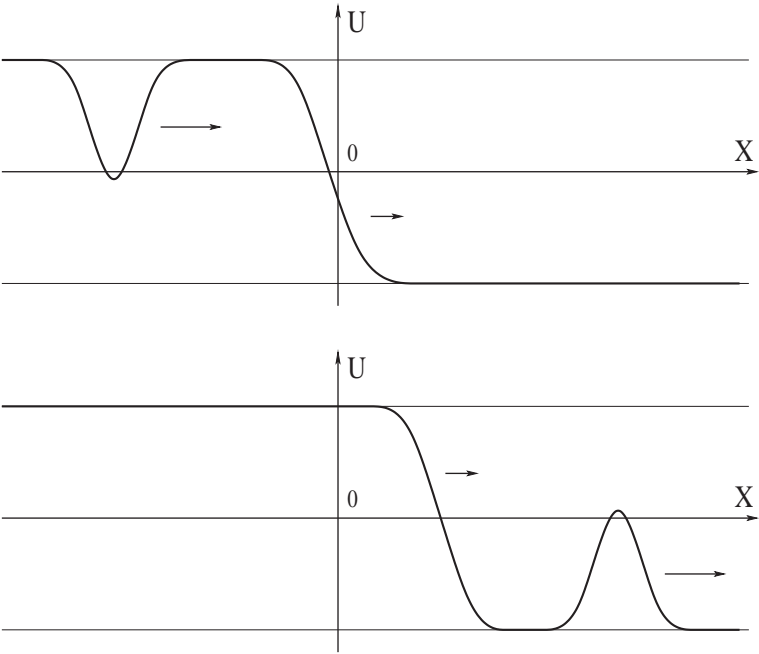

Fig. 22. Soliton "flip" after interacting with the "shock-wave" solution (54) for Eq. (52).

all the parts including (54), solitons and the "wave-train" will generically arise [73].

It's not difficult to understand also that for $|U_2| > |U_1|$ an additional step of the height $|U_2| - |U_1|$ with the decreasing steepness will arise near the level U_2 after the separation of solution (54) (Fig. 21).

We have to say now that the step-like initial conditions of the second type (the bottom of Fig. 19) can be investigated just by the change $U \rightarrow -U$.

Let us mention here also the very interesting solutions of (52) including the soliton part and solution (54). The soliton solutions coexist with solution (54) and the interaction of a soliton with (54) results in the phase shift and the soliton "flip" (Fig. 22).

Finally, we point out again that while considerations above were given for the function $U(X)$, representing Riemann invariants $r^{(1,2)}(X)$, we can express the results in terms of physical variables ρ and k using Eq. (24) (we also remind the readers that our analysis assumes the limit $\rho \rightarrow 0$ and $k \rightarrow 0$). We find that for $|U_1| > |U_2|$ (Fig. 23) the case

$$U_1 \sim -U_2$$

corresponds to the case $\rho(X) > 0$, $k(X) > 0$. For $|U_1| - |U_2| \ll |U_1|$ we also have $\rho_2 \ll \rho_1$, $k_1 \ll k_2$ (see Fig. 23). It is not difficult to see that conditions of this type can arise naturally after separating the right- and left-moving parts of initial conditions, as shown in Fig. 24.
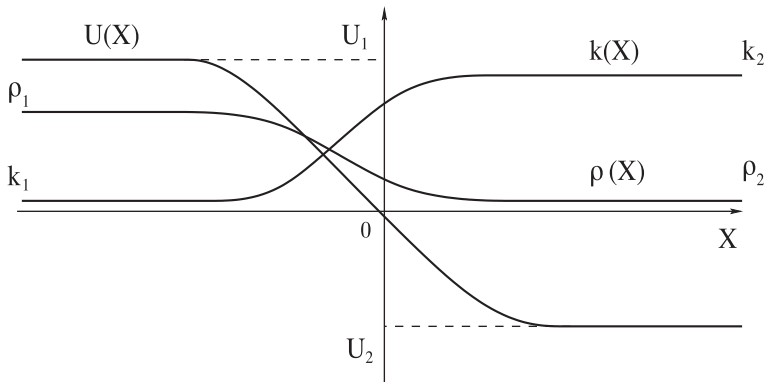
Fig. 23. Correspondence between functions $U(X)$ and $(\rho(X), k(X))$ in the left-moving part of the step-like initial conditions for $T > 0$.
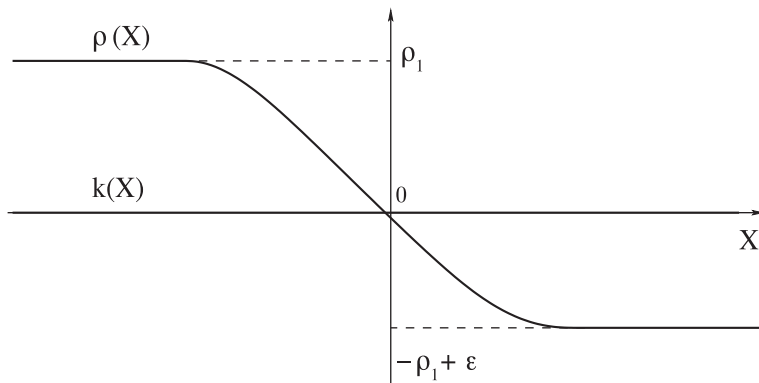
Fig. 24. Initial conditions for $\rho(X)$ and $k(X)$, which give rise to the case $U_1 \sim -U_2$, $|U_1| > |U_2|$, after separation of the left- and right-moving parts for $T > 0$.

References

[1] M.J. Ablowitz, H. Segur, Solitons and the Inverse Scattering Transform, Society for Industrial and Applied Mathematics (SIAM), Philadelphia, 1981.
[2] V. Ahufinger, A. Sanpera, P. Pedri, L. Santos, M. Lewenstein, Phys. Rev. A 69 (5) (2004) 053604.
[3] V. Ahufinger, A. Sanpera, Phys. Rev. Lett 94 (13) (2005) 130403.
[4] E. Altman, A. Polkovnikov, E. Demler, B.I. Halperin, M.D. Lukin, Phys. Rev. Lett. 95 (2) (2005) 020402.
[5] W. Bakr et al, Nature 462 (2009) 74.
[6] V.I. Bespalov, V.I. Talanov, JETP Lett. 3 (1966) 307.
[7] E. Bettelheim, A.G. Abanov, P. Wiegmann, Phys. Rev. Lett. 97 (2006) 246402. <arXiv:cond-mat/0607453>.
[8] E. Bettelheim, A.G. Abanov, P. Wiegmann, Phys. Rev. Lett. 97 (2006) 246401. <arXiv:cond-mat/0606778>.
[9] E. Bettelheim, A.G. Abanov, P. Wiegmann, J. Phys. A40 (2007) F193–F208. <arXiv:nlin/0605006>.
[10] L.A. Borgad, A.R. Its, V.B. Matveev, S.V. Manakov, V.E. Zakharov, Phys. Lett. 63A (N3) (1979) 05.
[11] I. Bloch, Nature Phys. 1 (2005) 23.
[12] Immanuel Bloch, Jean Dalibard, Wilhelm Zwerger, Rev. Mod. Phys. 80 (3) (2008) 885–964.
[13] I. Bloch, Science 319 (2008) 1202.
[14] S. Burger, K. Bongs, S. Dettmer, W. Ertmer, K. Sengstock, A. Sanpera, G.V. Shlyapnikov, M. Lewenstein, Phys. Rev. Lett. 83 (25) (1999) 5198–5201.
[15] Y. Castin, Eur. Phys. J. B 68 (2007) 556.
[16] A. Daley et al, J. Statist. Mech. Theory Expt. 2004 (4) (2004) 04005.
[17] B. Damski, J. Zakrzewski, L. Santos, P. Zoller, M. Lewenstein, Phys. Rev. Lett. 91 (8) (2003) 080403.
[18] J. Denschlag et al, Science 287 (2000) 97.
[19] V.S. Druma, JETP Lett. 19 (12) (1974) 219–225.
[20] L.-M. Duan, E. Demler, M.D. Lukin, Phys. Rev. Lett. 91 (9) (2003) 090402.
[21] B. Eiermann, Th. Anker, M. Albiez, M. Taglieber, P. Treutlein, K.-P. Marzlin, M.K. Oberthaler, Phys. Rev. Lett. 92 (23) (2004) 230401.
[22] L. Fallani, L. De Sarlo, J.E. Lye, M. Modugno, R. Saers, C. Fort, M. Inguscio, Phys. Rev. Lett. 93 (14) (2004) 140406.
[23] E. Fermi, J.R. Pasta, S. Ulam, Studies of nonlinear problems I., Los Alamos Report No. LA-1940, 1955.
[24] E. Fradkin, Field Theories of Condensed Matter Systems, Addison-Wesley Publishing Company, 1991.
[25] I.M. Gelfand, B.M. Levitan, Izvestia Akad. Nauk S.S.S.R. Ser. Math. 15 (1951) 309.
[26] N. Gemelke et al, Nature 460 (2009) 995.
[27] G.S. Gardner, J.M. Green, M.D. Kruskal, R.M. Miura, Phys. Rev. Lett. 19 (1967) 1095.
[28] T. Giamarchi, Quantum Physics in One dimension, Oxford Science Publishing, 2004.
[29] M. Greiner, S. Foelling, Nature 453 (2008) 736.
[30] M. Greiter, F. Wilczek, E. Witten, Mod. Phys. Lett. 3 (1989) 405.
[31] A.V. Gurevich, L.P. Pitaevskii, JETP Lett. 17 (1973) 193–195.
[32] A.V. Gurevich, L.P. Pitaevskii, Sov. Phys. JETP 38 (1974) 291–297.
[33] E. Haller et al, Science 325 (2009) 1224.
[34] B.I. Halperin, P.C. Hohenberg, Phys. Rev. 188 (1969) 898–918.
[35] D. Heine et al, New J. Phys. 12 (2010) 095005.
[36] S. Hofferberth et al, Nature Phys. 449 (2007) 324.
[37] S. Hofferberth et al, Nature Phys. 4 (2008) 489.
[38] S.D. Huber, E. Altman, H.P. Büchler, G. Blatter, Phys. Rev. B 75 (8) (2007) 085106.
[39] S.D. Huber, B. Theiler, E. Altman, G. Blatter, Phys. Rev. Lett. 100 (5) (2008) 050404.
[40] R. Jackiw, A. Kerman, Physics Letters A 71 (2–3) (1979) 158–162.
[41] D. Jaksch, P. Zoller, Ann. Phys. 315 (2005) 52.
[42] Magnus Johansson, Yuri S. Kivshar, Phys. Rev. Lett. 82 (1) (1999) 85–88.
[43] B.B. Kadomtsev, V.I. Petviashvili, Sov. Phys. Dokl. 15 (1970) 539–541.
[44] M. Karski, L. Förster, J.M. Choi, W. Alt, A. Widera, D. Meschede, Phys. Rev. Lett. 102 (5) (2009) 053001.
[45] I. Kay, H.E. Moses, Nuovo Cimento 3 (1956) 276;
    I. Kay, H.E. Moses, J. Appl. Phys. 27 (1956) 1503.
[46] P.G. Kevrekidis, R. Carretero-González, G. Theocharis, D.J. Frantzeskakis, B.A. Malomed, Phys. Rev. A 68 (3) (2003) 035602.
[47] I. Khalatnikov, V.V. Lebedev, J. Low Temp. Phys. 32 (1978) 789.
[48] L. Khaykovich et al, Science 287 (2002) 97.
[49] T. Kinoshita et al, Nature 440 (2006) 900.
[50] Yuri S. Kivshar, Boris A. Malomed, Rev. Mod. Phys. 61 (4) (1989) 763–915.
[51] A.B. Kuklov, B.V. Svistunov, Phys. Rev. Lett. 90 (10) (2003) 100401.
[52] Stefan Palzer, Christoph Zipkes, Carlo Sias, Michael Köhl, Phys. Rev. Lett. 103 (15) (2009) 150601.
[53] M.D. Kruskal, N.J. Zabusky, J. Math. Phys. 5 (2) (1964) 231–244.
[54] K. Krutitsky et al., 2010. <arXiv:0907.0625>.
[55] T. Lahaye et al, Rep. Progress Phys. 72 (2007) 126401.
[56] Jarrett Lancaster, Aditi Mitra, Phys. Rev. E 81 (6) (2010) 061134.
[57] P.D. Lax, Commun. Pure Appl. Math. 21 (1968) 467.
[58] P.D. Lax, C.D. Levermore, The small dispersion limit for the Korteweg–de Vries equation I, II, and III, Commun. Pure Appl. Math. 36 (1983) (253–290, 571–593, 809–830).
[59] P.D. Lax, C.D. Levermore, S. Venakides, The generation and propagation of oscillations in dispersive IVPs and their limiting behavior, Important Developments in Soliton Theory 1980–1990, Springer Series in Nonlinear Dynamics, Springer, Berlin, 1993. pp. 205–241.
[60] M. Lewenstein et al, Adv. Phys. 56 (2007) 243.
[61] V.A. Marchenko, Doklady. Akad. Nauk SSSR 104 (1955) 695.

[62] T. Maxworthy, L.G. Redekopp, Icarus 29 (1976) 261.
[63] J.W. Miles, J. Fluid Mech. 79 (1977) 171–179.
[64] R.M. Miura, J. Math. Phys. 9 (1968) 1202–1204.
[65] Jongchul Mun, Patrick Medley, Gretchen K. Campbell, Luis G. Marcassa, David E. Pritchard, Wolfgang Ketterle, Phys. Rev. Lett. 99 (15) (2007) 150604.
[66] V. Murg, F. Verstraete, J.I. Cirac, Phys. Rev. A 75 (3) (2007) 033605.
[67] P.I. Naumkin, I.A. Shishmarev, Funct. Anal. Appl. 25 (1) (1991) 16–25.
[68] K. Nelson, X. Li, D. Weiss, Nature Phys. 3 (2007) 556.
[69] A.C. Newell, Solitons in Mathematics and Physics, Society for Industrial and Applied Mathematics, 1985.
[70] S.P. Novikov, S.V. Manakov, L.P. Pitaevskii, V.E. Zakharov, Theory of Solitons. The Inverse Scattering Method, Plenum, New York, 1984.
[71] L. Ostrovsky, A. Potapov, Modulated Waves Theory and Applications, The Johns Hopkins University Press, 1999.
[72] H. Ott et al, Nature Phys. 4 (2008) 949.
[73] T.L. Perelman, A. Kh. Fridman, M.M. Yelyashevich, Sov. Phys. JETP. 39 (1974) 643–646.
[74] L. Pitaevskii, S. Stringari, Bose–Einstein Condensation, Oxford Science Publications, 2002.
[75] A. Polkovnikov, E. Altman, E. Demler, B. Halperin, M.D. Lukin, Phys. Rev. A 71 (6) (2005) 063613.
[76] Stephan Ritter, Anton Öttl, Tobias Donner, Thomas Bourdel, Michael Köhl, Tilman Esslinger, Phys. Rev. Lett. 98 (9) (2007) 090402.
[77] N.N. Romanova, Theor. Math. Phys. 39 (2) (1979) 415–421.
[78] J. Satsuma, J. Phys. Soc. Japan. 40 (1976) 286–290.
[79] L. Sadler et al, Nature 443 (2006) 312.
[80] R.T. Scalettar, G.G. Batrouni, A.P. Kampf, G.T. Zimanyi, Phys. Rev. B 51 (13) (1995) 8467–8480.
[81] V.W. Scarola, S. Das Sarma, Phys. Rev. Lett. 95 (3) (2005) 033003.
[82] U. Schneider et al., Breakdown of diffusion: from collisional hydrodynamics to a continuous quantum walk in a homogeneous Hubbard model, 2010. <arXiv:1005.3545>.
[83] Guido Schmid, Synge Todo, Matthias Troyer, Ansgar Dorneich, Phys. Rev. Lett. 88 (16) (2002) 167208.
[84] U. Schollwöck, Rev. Mod. Phys. 77 (1) (2005) 259–315.
[85] Sherson et al, Nature 467 (2010) 68.
[86] Niels Strohmaier, Daniel Greif, Robert Jördens, Leticia Tarruell, Henning Moritz, Tilman Esslinger, Rajdeep Sensarma, David Pekker, Ehud Altman, Eugene Demler, Phys. Rev. Lett. 104 (8) (2010) 080401.
[87] B. Sutherland, Beautiful Models, World Scientific, 2004.
[88] Andrea Trombettoni, Augusto Smerzi, Phys. Rev. Lett. 86 (11) (2001) 2353–2356.
[89] S. Trotzky et al, Science 319 (2008) 295.
[90] M. Wadati, J. Phys. Soc. Japan 34 (1973) 1289.
[91] X.G. Wen, Adv. Phys. 44 (1995) 405.
[92] Biao Wu, Qian Niu, Phys. Rev. A 64 (6) (2001) 061603.
[93] Alexey V. Yulin, Dmitry V. Skryabin, Phys. Rev. A 67 (2) (2003) 023611.
[94] N.J. Zabusky, Phenomena Associated with the oscillations of a Nonlinear Model String, in: Stefan Drobot (Ed.), Proceedings of the Conference on Mathematical Models in the Physical Sciences, Prentice-Hall Inc., New York, 1963, p. 99.
[95] N.J. Zabusky, M.D. Kruskal, Phys. Rev. Lett. 15 (6) (1965) 240–243.
[96] V.E. Zakharov, S.V. Manakov, Sov. Phys. JETP 44 (1) (1976) 106–112.
[97] V.E. Zakharov, A.B. Shabat, Sov. Phys. JETP 37 (1973) 823–828.
[98] V.E. Zakharov, A.B. Shabat, Funk. Anal Pril. 8 (3) (1974) 43–53.
[99] Jakub Zakrzewski, Phys. Rev. A 71 (4) (2005) 043601.
[100] Zimmermann et al., 2010. <arXiv:1011.1004>.